Mathematical Models of Immune Responses Following Vaccination with Application to Brucella Infection

Mirjam Sarah Kadelka

Thesis submitted to the Faculty of the
Virginia Polytechnic Institute and State University
in partial fulfillment of the requirements for the degree of

Master of Science
in
Mathematics

Stanca M. Ciupe, Chair
Eric de Sturler
Shu-Ming Sun

May 5, 2015
Blacksburg, Virginia

Keywords: Brucella Abortus, Mathematical Modeling, Vaccination

Mathematical Models of Immune Responses Following Vaccination with Application to Brucella Infection

Mirjam Sarah Kadelka

(ABSTRACT)

For many years bovine brucellosis was a zoonosis endemic in large parts of the world. While it is still endemic in some parts, such as the Middle East or India, several countries such as Australia and Canada have successfully eradicated brucellosis in cattle by applying vaccines, improving the hygienic standards in cattle breeding, and slaughtering or quarantining infected animals. The large economical impact of bovine brucellosis and its virulence for humans, coming in direct contact to fluid discharges from infected animals, makes the eradication of bovine brucellosis important to achieve. To achieve this goal several vaccines have been developed in the past decades. Today the two most commonly used vaccines are Brucella abortus vaccine strain 19 and strain RB51. Both vaccines have been shown to be effective, but the mechanisms of immune responses following vaccination with either of the vaccines are not understood yet. In this thesis we analyze the immunological data obtained through vaccination with the two strains using mathematical modeling. We first design a measure that allows us to separate the subjects into good and bad responders. Then we investigate differences in the immune responses following vaccination with strain 19 or strain RB51 and boosting with strain RB51. We develop a mathematical model of immune responses that accounts for formation of antagonistic pro and anti-inflammatory and memory cells. We show that different characteristics of pro-inflammatory cell development and activity have an impact on the number of memory cells obtained after vaccination.

Contents

List of Figures

List of Tables

Chapter 1

Introduction

This thesis is structured as follows. Chapter two presents a brief introduction of the biology of the immune system, and in particular describes the switch between Th_1 and Th_2 immune responses, that can be observed in many infections. We follow that with an overview of vaccination, its origin and different vaccination strategies applied today. Lastly, we describe the brucella infection in cattle, caused by the bacterium Brucella abortus, and give a brief overview on different vaccines used in eradication programs against brucellosis. In chapter three we give a short mathematical overview on equilibria and their stability, and introduce different mathematical techniques that can be used to model interactions of populations participating in immune responses. We then present previous modeling work on the switch between Th_1 and Th_2 immune responses. We briefly describe two models which we later use to create our own model(s) of the immune reaction following a vaccination against brucellosis in cattle. In chapter four, we investigate the influence of two different vaccine strategies on the immune response after vaccination against brucellosis, applying techniques from statistics to data obtained from [13]. In chapter five, we formulate an ODE model for the immune cells' development and function based on the data described in chapter four. We analyze the model and show that the solutions are positive and bounded. Moreover, we give conditions for the existence and stability of steady-states. We then investigate the influence of different parameters on the size of memory cell population at steady-state. In chapter six we conclude this thesis by giving a brief outlook on our future work, which relates the cellular interactions with cytokine levels.

Chapter 2

Biological Background

2.1 The Immune System

The term immune system condenses all processes and components in the body that are involved in the defense against a pathogen, a particle recognized as foreign to the body. It therefore includes organs, different cell types and various other components such as cytokines and chemokines. It can be seen as the body's defense line against infections. The immune system can be divided into two main components, the innate immune system responsible for a rapid and not pathogen-specific defense and the adaptive immune system which is pathogen-specific and includes memory.

The innate immune response mainly consists of inflammatory responses and phagocytic responses in which pathogens are eaten by cells such as neutrophiles and macrophages [1]. By digesting the pathogens and presenting its peptides on their cell surface they become antigen-presenting cells (APC) that initiate the adaptive immune responses.

Adaptive immune responses, driven by lymphocytes, can also be split up into two components. The antibody (or humoral) response, in which B lymphocytes play an important role, and the cell-mediated immune response [1], executed by T lymphocytes. Immature or naive versions of both B and T cells can be found in large numbers in the lymph nodes.

2.1.1 Cell mediated Immune Response

The cell mediated immune response is responsible for the annihilation of pathogens that survive the killing mechanisms inside host cells such as macrophages. It involves two subgroups of T lymphocytes: the CD4 and CD8 T cells.

Immature dendritic cells ingest the pathogen and become activated. They mature, present different peptide complexes of the pathogen's antigens on their surface and travel to the lymph nodes. After degrading the antigen inside the cell so called major histocom-

patible complexes (MHC) bind to the antigen peptides and travel to the cell surface where the MHC-peptide complex is presented. There are two structurally and functionally distinct MHC proteins, class I MHC proteins and class II MHC proteins [1].

Naive CD4 T cells in the lymph nodes react towards the encountering of MHC class II peptide complexes and start differentiating into T helper cells via two different pathways resulting in either Th_1 or Th_2 cells. As suggested by their name T helper cells mainly execute supportive functions. Th_1 cells secrete pro-inflammatory cytokines [24] such as Interferon-γ (IFN-γ) and tumor necrosis factor α (TNF-α) which cause reactions in infected cells, that lead to their destruction. They also support macrophage activation and CD8 T cell differentiation [31]. For these reasons they play an important role in battling against intracellular pathogens. Th_2 cells produce a distinct set of anti-inflammatory [24] cytokines such as Interleukin-4 (IL-4), Interleukin-5 (IL-5) and Interleukin-13 (IL-13) that are inducing a strong antibody production. They are therefore important in the antibody-mediated immune response against extracellular pathogens and in anti-inflammatory immune response antagonizing the inflammatory immune response.

Naive CD8 T cells bind to class I MHC-peptide complexes [31] and differentiate into cytotoxic CD8 T cells also called T killer cells. Cytotoxic CD8 T cells secrete toxins such as perforin and granzymes into chronically infected cells in order to kill them.

In the cell mediated immune response an infected host cell communicates, via antigen presentation, its infection to T helper cells which, in consequence, recruit cytotoxic T cells to destroy the infected cell before the pathogen can replicate inside the cell. A diagram of the cellular immune responses is shown below (see Figure 2.1).

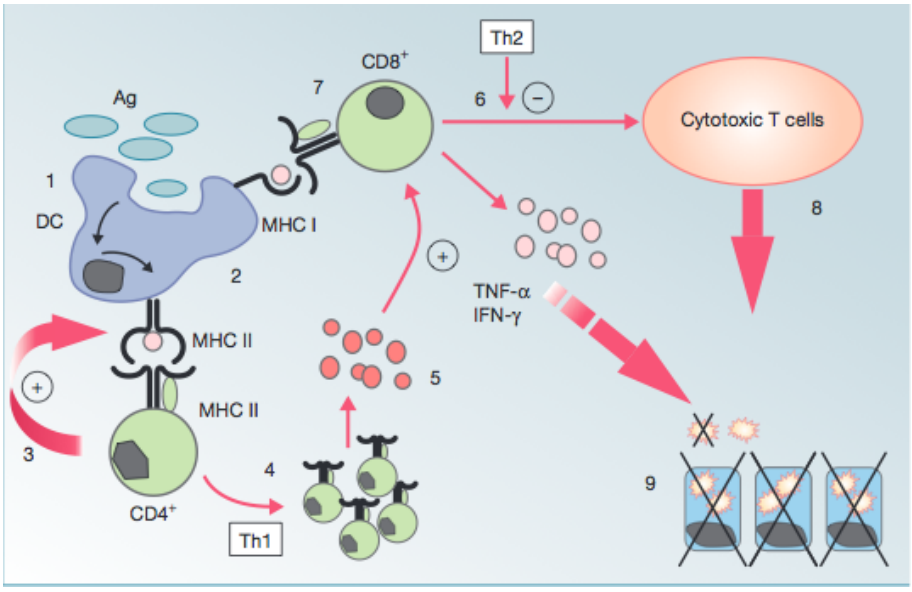

Figure 2.1: Cell mediated immune response [31]

During the cellular immune response memory cells are developed. Most of the effector T cells die of apoptosis within a few days [31] whereas a few differentiate into long living memory T cells. The persistence of memory cells after the eradication of the pathogen leads to an improved ability of the immune system to fight the pathogen upon reencountering it. The secondary immune response is greater in magnitude, faster and more sensitive to lower doses of antigen compared to the primary response [18]. This development of memory cells is therefore the reason why the body has lifelong immunity to many common infectious diseases after an initial exposure to the pathogen [1]. It is the underlying concept behind vaccination.

2.1.2 Humoral Immune Response

Upon encounter with an APC, naive T cells that differentiate to become Th_2 cells help immature B lymphocytes become activated and differentiate into either antibody secreting plasma cells [19] or long living memory B cells. These memory B cells can rapidly produce antigen-specific antibodies upon a renewed encounter with the same or a closely related pathogen. The antibodies produced by the plasma cells then bind to pathogens, thereby either neutralizing them or signaling phagocytic cells who ingest and destroy the antibody-pathogen complexes [19].

2.2 Vaccination

Vaccination is a method applied to build up protection against a disease in humans or animals by using the ability of the immune system to faster recognize and respond to known pathogens. The basic idea is to educate the immune response to respond to the pathogen in a controlled way, e.g. by administering a weakened form of the pathogen that the immune system is able to fight off before the pathogen can cause disease. Upon the secondary encounter with the pathogen, memory cells produced in response to the vaccination are reactivated into effector cells. These cells start removing the pathogen at a faster rate.

Even though there have been attempts of vaccinations before him [26], Edward Jenner is commonly considered the founder of the practice of vaccination. Today we have successful vaccination programs against an array of pathogens such as measles, mumps and rubella [25] and hepatitis B [10].

2.2.1 Vaccination with booster

Many vaccines such as the one against the hepatitis B virus or against measles do not induce long-lasting protection after the first dose. For most vaccines there is a need for a second, sometimes even a third vaccination, called booster. Boosters can be seen as reminders to the

immune system. In general each booster extends the time protection lasts. There are also some vaccines that require to be administered repeatedly, e.g. the tetanus vaccine every ten years, in order to ensure protection.

Fighting-off intracellular pathogen is supposed to require a strong cell-mediated immune response. Repeated administration of the same vaccine, called homologous boosting, is often a good way to optimize the humoral immune response while it usually lacks the ability of improving the cell-mediated immune response. Heterologous prime-boost immunization, where the antigen is administered in different forms in the primary and booster vaccine have been shown to be highly effective for enhancing humoral and cellular mediated immunity [12]. For example vaccinating with a live vaccine and boosting with an adenovirus against tuberculosis has been shown to induce an enhanced cellular immune response compared to homologous prime-boost vaccination just using the live vaccine [21].

In this thesis we investigate possible differences of homologous and heterologous boosting in vaccination against brucellosis, a disease that is caused by bacteria and mainly occurs in cattle and other ruminants.

2.3 Th_1 - Th_2 Switch

As described in 2.1.1, naive CD4 T cells undergo two distinct pathways of differentiation resulting in either Th_1 or Th_2 cells with characteristic sets of cytokines. Th_1 cytokines are often referred to as pro-inflammatory cytokines while Th_2 cytokines are counteracting anti-inflammatory cytokines. The main pro-inflammatory cytokine is IFN-γ. It is not only produced by Th_1 cells but also enhances the differentiation of naive CD4 T cells into Th_1 cells. Without any counteracting forces, this self promotion leads to an autoimmune reaction. As a result, the immune response turns against healthy cells, thereby causing serious inflammations and tissue damages. The antagonists to the inflammatory Th_1 cytokines are the anti-inflammatory Th_2 cytokines led by IL-4. They inhibit the differentiation of naive CD4 T cells into Th_1 cells while promoting the differentiation into Th_2 cells. Another important subpopulation of CD4 T cells in this context are the regulatory T cells. These cells suppress the immune system by inhibiting the differentiation of naive CD4 T cells into effector cells. In summary we have self promotion in either of the two T helper cell subpopulations and cross-inhibition between them. Additionally both populations are inhibited by regulatory CD4 T cells.

For a long time it was believed that T helper cell differentiation is linear and irreversible [11]. However, recent studies show that the spectrum of cytokines a T helper cell produces is not as stable as it was thought to be and that T helper cells can change their phenotypes. E.g. in [17] it has been shown that, given certain stimuli, Th_2 cells produce IFN-γ, a cytokine usually produced by Th_1 cells.

Often the course of a disease can be related to whether the inflammatory Th_1 or the anti-inflammatory humoral Th_2 response is predominant. In chronic infections we usually see a strong inflammatory immune response at the beginning. This response is lost over time

of infection as a pathogen-specific antibody response appears and the disease reaches clinical stages [23]. In other cases, such as allergies, we see a switch from Th_2 to Th_1 response. These switches from Th_1 to Th_2 response or vice-versa have been subject to several studies such as [22] and [29]. We will take a closer look at some of them in the following chapter.

2.4 Brucella Abortus

Brucella abortus is an bacterium causing a chronic disease called brucellosis. The bacterium can be mainly found in cattle, bison and buffalo populations but it is also pathogenic to other species and humans. Brucella abortus is an intracellular bacterium that survives and replicates in host macrophages [30]. It also has the ability to inhibit apoptosis of the macrophages [16], that is the programmed self-destruction of infected macrophages. In cattle, Brucella abortus causes abortions and stillbirths [3] which can become a major economical problem. The disease is usually transmitted by ingestion of food or water that was in contact with placenta, fetus, fetal fluids or vaginal discharges from infected animals [3]. Due to the large economical impact of the disease many countries have performed or are still performing eradication programs. Parts of these programs are precautionary vaccination of cattle with either of the two available vaccines, strain 19 or strain RB51. Both vaccines are live attenuated vaccines, meaning that they are derived from disease causing bacteria that have been weakened under laboratory conditions. Usually these vaccines do not cause disease. However, in pregnant cattle both strains can cause abortions [4]. Therefore the vaccine should be administered during calfhood. Vaccine strain 19 is more virulent than strain RB51 [4] but both strains can infect humans which is why safety precautions such as wearing gloves, glasses and a mask must be taken when handling the vaccines [13]. Also, in contrast to vaccine strain 19, strain RB51 does not lead the immune system to produce antibodies that can be detected in serological test used to diagnose brucellosis in cattle [33]. This makes the distinction between infected and vaccination animals and the decision which animals have to slaughtered or quarantined easier.

In many countries, especially the more developed ones, brucellosis is relatively well controlled. Contrarily, in other parts of the world, such as the Mediterranean, Middle East, Latin America and parts of Asia [32], it is still an uncontrolled problem. In India, there are hardly any restrictions on the trade of farm animals. Often local cattle yards and fairs are used for trading [32]. Additionally artificial inseminations are performed using semen from bulls that are not tested on brucellosis and in average the hygiene standards in the farms are very low. These are several factors leading to a wide spread of brucellosis in India since healthy animals are likely to come into contact with contagious material. In order to eradicate or at least control the spread of brucellosis in India and other countries with similar farming standards it is crucial to perform mass vaccinations along with a change in the handling of farm animals.

Our interest in studying brucella abortus vaccination was started by interactions with Dr. Sriranganathan from the Virginia Tech veterinary school who is collaborating with Dr.

Dorneles and Dr. Lage from Universidade Federal de Minas Gerais in Brazil to investigate immune responses following vaccination against brucellosis in cattle. In [14] Dorneles et al. evaluate the effects of strain 19 vaccination and strain RB51 boosting on CD4 and CD8 T cell proliferation and IFN-γ and IL-4 production by T lymphocytes in cattle. They find that CD4 and CD8 T lymphocytes both proliferate in response to vaccination with strain 19. They also show that most of the IFN-γ produced after strain 19 vaccination and RB51 boosting is expressed by CD4 T cells. Their study also reveals that the booster vaccination with strain RB51 does not significantly enhance the immune response compared to just vaccinating with strain 19. Additionally they conclude from their data that IL-4 does not play a significant role in building up immunity against brucellosis in response to vaccination.

We obtained two datasets from studies investigating the immune response in cattle following vaccination. In the first set data are gathered from cows vaccinated with strain 19 vaccine and revaccinated with strain RB51 vaccine whereas in the second the initial vaccination and the booster are both performed using strain RB51.

Chapter 3

Mathematical Background

3.1 Introduction

Many scientific fields model their underlying processes using mathematical tools. The mathematical models can be systems of ODEs, PDEs, SDEs, etc. and can involve large numbers of equations and parameters. Such large systems are reduced to an often astonishing small set of equations, describing only the key processes, while still remaining able to simulate the dynamical behavior of the system. Mathematical modeling is used in biological application to gain a further understanding of the key processes that govern the dynamics of a system, or to estimate parameters that are hard or not possible to determine in experiments. Another and probably the most important use of mathematical models is to predict a system's dynamics under new conditions and, thereby, gain insight in what might be worth testing experimentally. Some techniques used in mathematical modeling such as mass-action type interactions, Lotka-Volterra type competition models, stability analysis and bifurcation will be briefly introduced in this section.

We will motivate the use of mathematical models to explain $Th_1 - Th_2$ switch in brucellosis by giving a short overview of previous modeling work on immune responses in diseases that result in switches between inflammatory Th_1 and anti-inflammatory Th_2 responses.

3.2 Equilibria and Stability

Let us consider an autonomous system

$$\frac{dx}{dt} = X(x), \tag{3.1}$$

i.e. a system of n ordinary differential equations describing the dynamics of n populations $x_1, \ldots, x_n$, where the equations do not depend on the independent variable, say t. Further-

more we assume that all functions $X_i(x)$, $i = 1, \ldots, n$, and their first derivatives with respect to x_j, $j = 1, \ldots, n$, are continuous functions of $x_1, \ldots, x_n$. An important property of such systems is the following:

Lemma 1. *The initial value problem*

$$\frac{dx}{dt} = X(x), \ x(t_0) = x_0,$$

with the properties described after (3.1) has a unique solution for any initial value $x_0 \in \mathbb{R}^n$ on a maximal interval $[t_0, b)$, where $b > t_0$ depends on x_0. If $b < \infty$, then the solution is unbounded.

Proof. This is a reformulation of Theorem 1, p.177 in [2].
The proof of a more general result can be found in [7], Theorem 2, page 172 and Corollary 1, page 173. □

Definition 1. *We call a solution $\overline{x}$ of the equation*

$$X(x) = 0 \tag{3.2}$$

an equilibrium or steady-state of the system.

According to their definition, equilibria are the states of the system that once reached are not left anymore.

In the context of equilibria there are questions regarding their stability. E.g. what happens to a system starting in close proximity of a steady-state. Is it attracted by the steady-state in which case we call the equilibrium stable or is it traveling away from it and we would therefore call the steady-state unstable.

The following two definitions are reformulations of definitions 5.2, page 178 and 5.3, page 179 in [2].

Definition 2. *An equilibrium solution $\overline{x}$ of $\frac{dx}{dt} = X(x)$ is called locally stable if for each $\epsilon > 0$ there exists a $\delta > 0$ such that for every solution $x(t)$ of $\frac{dx}{dt} = X(x)$ with initial condition $x(t_0) = x_0$ with the property*

$$\|x_0 - \overline{x}\|_2 < \delta$$

satisfies the condition

$$\|x(t) - \overline{x}\|_2 < \epsilon$$

for all $t \geq t_0$. If the equilibrium solution is not locally stable it is said to be unstable.

Definition 3. *An equilibrium solution $\overline{x}$ of $\dfrac{dx}{dt} = X(x)$ is called locally asymptotically stable if it is locally stable and if there exists $\gamma > 0$ such that if*

$$\|x_0 - \overline{x}\|_2 < \gamma,$$

then

$$\lim_{t\to\infty} \|x(t) - \overline{x}\|_2 = 0.$$

Next we want to get a condition that guarantees that a system is locally asymptotically stable. Therefore we first introduce the Jacobian or Jacobian matrix of a system.

Definition 4. *The matrix $J \in M^{n\times n}$ with*

$$J_{i,j} = \frac{\partial X_i}{\partial x_j}, \qquad i,j \in \{1,\dots,n\},$$

is called Jacobian or Jacobian matrix of the system $\dfrac{dx}{dt} = X(x), x = (x_1,\dots,x_n)$.

Definition 5. *Let $A \in M^{n\times n}$, where M is a field (such as $\mathbb{R}$ or $\mathbb{C}$). The characteristic polynomial $P_A(\lambda)$ of A is*

$$P_A(\lambda) = \det(\lambda I_n - A) = 0 \tag{3.3}$$

where I_n is the identity matrix of order n. The characteristic polynomial can also be written in the form

$$P_A(\lambda) = \det(A - \lambda I) = \lambda^n + a_1\lambda^{n-1} + \ldots + a_{n-1}\lambda + a_n,$$

where the coefficients a_i, $i = 1,\dots,n$, are elements of M. Solutions of (3.3) are called eigenvalues of the matrix A.

Lemma 2 (Ruth-Hurwitz Criterium)**.** *Given the polynomial*

$$P(\lambda) = \lambda^n + a_1\lambda^{n-1} + \ldots + a_{n-1}\lambda + a_n$$

where the coefficients a_i, $i = 1,\dots,n$, are real constants, define the n Hurwitz matrices

$$H_1 = \begin{pmatrix} a_1 \end{pmatrix},\ H_2 = \begin{pmatrix} a_1 & 1 \\ a_3 & a_2 \end{pmatrix},\ H_3 = \begin{pmatrix} a_1 & 1 & 0 \\ a_3 & a_2 & a_1 \\ a_5 & a_4 & a_3 \end{pmatrix},$$

and

$$H(n) = \begin{pmatrix} a_1 & 1 & 0 & 0 & \dots & 0 \\ a_3 & a_2 & a_1 & 1 & \dots & 0 \\ a_5 & a_4 & a_3 & a_2 & \dots & 0 \\ \vdots & \vdots & \vdots & \ddots & \dots & \vdots \\ 0 & 0 & 0 & 0 & \dots & a_n \end{pmatrix},$$

where $a_j = 0$ *if* $j > n$.
All of the roots of $P(\lambda)$ *are negative or have negative real part iff the determinant of all Hurwitz matrices are positive:*

$$\det H_j > 0, \quad j = 1, 2, \ldots, n.$$

Proof. This lemma is obtained from Theorem 4.4., page 150 in [2]. □

Knowing this condition we can now state the following:

Lemma 3. *Let* $\overline{x}$ *be an equilibrium solution of a nonlinear first-order autonomous system* $\frac{dx}{dt} = X(x)$ *as described after (3.1) and let* $J(\overline{x})$ *be the Jacobian evaluated at* $\overline{x}$. *If the characteristic polynomial of the Jacobian matrix* $J(\overline{x})$ *satisfies the conditions of the Ruth-Hurwitz criterium, that is, the determinants of all Hurwitz matrices are positive,*

$$\det(H_j) > 0, \ j = 1, \ldots, n,$$

then the equilibrium solution $\overline{x}$ *is locally asymptotically stable. If*

$$\det(H_j) < 0 \text{ for some } j \in \{1, \ldots, n\},$$

then the equilibrium $\overline{x}$ *is unstable.*

Proof. Reformulation of Theorem 5.5., page 190 in [2]. □

3.3 Bifurcation analysis

Bifurcation analysis investigates how varying a parameter in a system influences the dynamics of the sytem. The varied parameter is called bifurcation parameter. As the bifurcation paramater varies, the stability of a steady-state can change or new steady-states can occur. The parameter value at which such a change occurs is called bifurcation value [2]. There are several types of bifurcation such as saddle node, pitchfork and transcritical bifurcation [2]. We will focus on transcritical bifurcation as we will later see this type of bifurcation in our model. When a system has two steady states, one stable and one unstable, that collide at a certain value of the bifurcation parameter and exchange stability, this is called transcritical bifurcation. An example can be seen in Figure 3.1. At the bifurcation value 5 the two steady states collide and exchange stability.

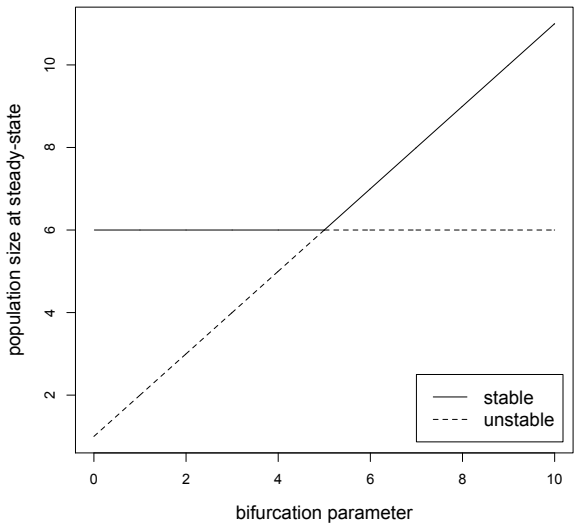

Figure 3.1: Transcritical bifurcation

3.4 Modeling techniques

Ordinary (ODE), partial (PDE) and stochastic (SDE) differential, and difference equations are common means used in modeling population growth and interactions between populations. They describe the dynamical interactions between variables of interest based on given biological assumptions. We will focus on ODE models and describe interactions of the following types below: mass action and Lotka-Volterra.

3.4.1 Modeling mass-action type interactions

Originating in chemistry to describe the dynamics of systems of chemical reactions, mass-action kinetics have numerous analytic properties of inherent interest from a dynamical systems perspective [9]. Mass-action is describing an interaction between two (or more) populations where the rate of change of the end product is proportional to the product of the amounts (densities or concentrations) of interacting populations. Assume, for example, that the rate of differentiation of naive CD4 T cells, N, into Th_1 cells is dependent on their interaction with activated macrophages, Φ. Then, a mass-action model describing this is

$$\frac{dN}{dt} = -\delta N \Phi,$$

where δ is the constant of proportionality.

3.4.2 Modeling competition: Lotka-Volterra

In many cases two or more populations considered in a model are competing for the same resource. Assume two populations, x and y, grow without influencing each other. This can be modeled by logistic growth:

$$\frac{dx}{dt} = r_x x \left(1 - \frac{x}{K_x}\right),$$
$$\frac{dy}{dt} = r_y y \left(1 - \frac{y}{K_y}\right),$$

where $K_x > 0$ and $K_y > 0$ are the carrying capacities, the maximal population sizes. $r_x > 0$ and $r_y > 0$ are called maximal per capita growth rates [34]. Logistic growth in which a population grows or decays towards its carrying capacity fits many observed populations.

Assume, that the carrying capacity is a shared resource [34] that the two populations x and y compete for. Then the presence of each inhibits the growth the other. We model this by

$$\frac{dx}{dt} = r_x x \left(1 - \frac{x + \alpha_y y}{K_x}\right),$$
$$\frac{dy}{dt} = r_y y \left(1 - \frac{y + \alpha_x x}{K_y}\right),$$

where all parameters are positive constants. This is called Lotka-Volterra competition model and can can also be applied for competition of more than two competing populations.

3.5 Previous modeling work on the Th_1-$Th2$ switch

3.5.1 A cytokine dependent model used to describe allergic reactions

An allergic reaction towards an allergen is characterized by an abnormal antibody mediated (Th_2-type) immune response and a comparably weak antagonizing inflammatory (Th_1-type) immune response. The principal idea of allergy treatment via hyposensitization is to increase the ratio of Th_1 versus Th_2 response. It is therefore important to understand which parameters drive naive CD4 T cells to differentiate in either of the two helper T cells. In [5] and subsequent publications [29] and [15], a mathematical model to describe the regulation of Th_1 versus Th_2 responses is introduced. It explains the dynamics of naive CD4 T cells, N, Th_1 and Th_2 cells, T_1, T_2, cytokines produced by Th_1 and Th_2 cells, IF and IL, respectively, and allergen in form of allergen presenting cells, A.

The model proposed in [29] does not consider cytokines explicitly since cytokines are

short lived compared to T cells [5]. Therefore production of IL is proportional to the concentration of Th_2 cells,

$$IL \propto T_2,$$

while the secretion of IF by Th_1 cells is supressed by IL and therefore [6]

$$IF \propto \frac{T_1}{1 + \text{ const } IL}.$$

The model equations are as follows [29]:

$$\begin{aligned}
\frac{dN}{dt} &= -N + \alpha - NA\left(\frac{T_1}{1+\mu_2 T_2} + c\right) - \phi NA(T_2 + c),\\
\frac{dTh_1}{dt} &= -T_1 + \nu NA\left(\frac{T_1}{1+\mu_2 T_2} + c\right),\\
\frac{dTh_2}{dt} &= -T_2 + \nu\phi NA\frac{T_2 + c}{1 + \mu_1 \frac{T_1}{1+\mu_2 T_2}},\\
\frac{dA}{dt} &= w(t) - A(T_1 + T_2).
\end{aligned} \tag{3.4}$$

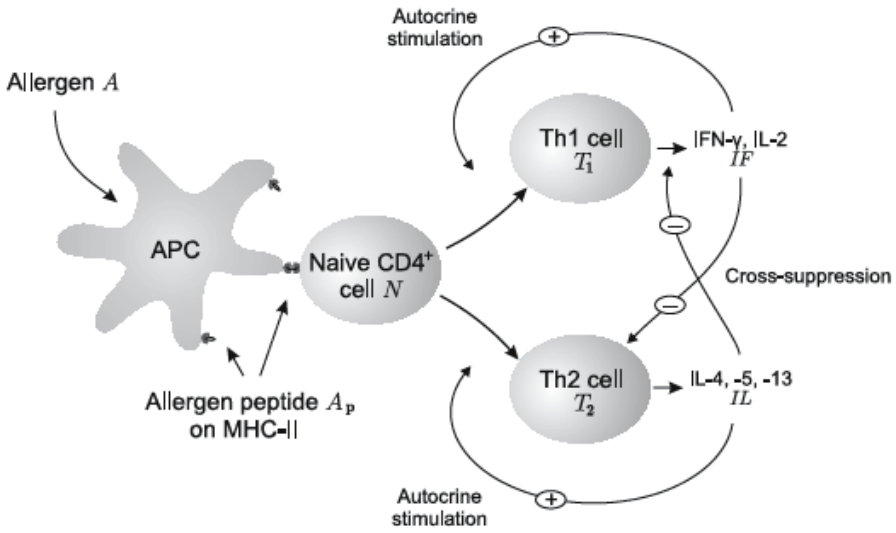

Figure 3.2: Scheme of interactions described in system (3.4) [6]

Naive CD4 T cells are produced at a rate α and proliferate at a rate ν. $w(t)$ represents the rate at which antigen presenting cells A present antigen after an allergen injection [6]. The parameters μ_1 and μ_2 are controlling the cross-suppression of Th_1 and Th_2 cells, while parameter ϕ is regulating self promoting effects in this system. Finally, parameter c is

implemented to represent a small cytokine background [6], to account for cytokines produced by cells other than T helper cells. A schematic view of the processes modeled in (3.4) is given in Figure 3.2

By investigating this system for a constant allergen supply, $w(t) = w$, the authors find two steady-states of this system. One steady-state represents high Th_1 and low Th_2 levels, while the other shows the opposite behavior. Next, they considered single high-dose antigen injections with dose D_p. To account for the short duration of an injection they assumed $w(t) = D_p\delta(t)$, where $\delta(t)$ is the Dirac delta function [29]. They investigated for which initial conditions of Th_1 and Th_2 cells a single high-dose injection of allergen does not change the Th_1/Th_2 ratio. Using these values as a separatix they divided the $Th_1 - Th_2$ plane into regions where an injection increases (white region in Figure 3.3) or decreases (grey region) the Th_1/Th_2 region.

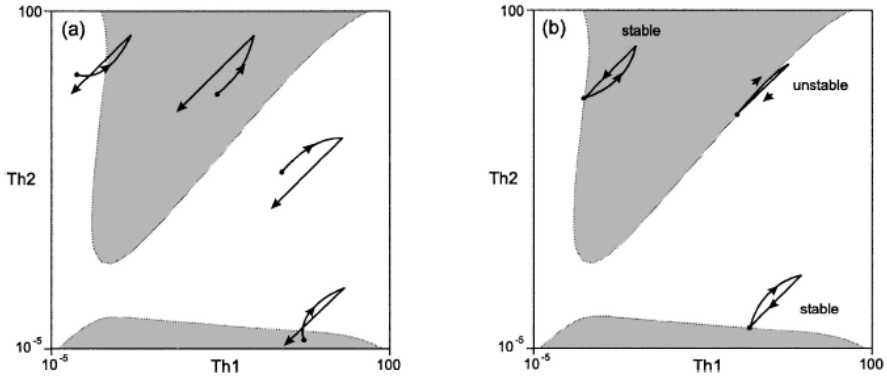

Figure 3.3: Separation $Th_1 - Th_2$ plane [29]

For initial conditions lying on the separatix, the trajectory will, after some time Δt, recross the initial point [29]. So repeating the injections with period Δt elicits a periodic behavior of this system and gives rise to new attractors whose location in the $Th_1 - Th_2$ plane depends on the period Δt. Panel (b) in Figure 3.3 shows three cyclic trajectories belonging to the same period Δt [29]. The authors' next goal is to determine how the period influences whether the system is approaching a state governed by Th_1, indicating the success of the therapy, or a state governed by Th_2. They found that there are three different regions of possible initial conditions in the $Th_1 - Th_2$ plane for which this question has to be answered separately. For all initial conditions they assume the ratio Th_1/Th_2 to be less than one, indicating an allergic individual. For initial conditions in the first region the Th_1/Th_2 ratio is continuously increasing independent of the choice of Δt. The second region contains all initial conditions for which an injection eventually leads to a decrease in the ratio, but the trajectory transiently crosses the separatix. Choosing the period such that the next injection is applied while the trajectory is still on the other side of the separatix leads to an increase of the ratio. The further the distance between the initial condition and the separatix,

the shorter the trajectory is on the other side of the separatix and the more difficult it is to find an appropriate period. The third region assembles all initial conditions for which the trajectory never crosses the separatix. In this case any injection further decreases the Th_1/Th_2 ratio. Taking these results we can see how this model can be used to test variations of hyposensitization strategies to optimize therapies.

When studying the immune response occurring after vaccination against brucellosis, we derived a cytokine dependent model for the CD4 T cells, that builds on model (3.4) and an extended version derived in [15].

3.5.2 Th_1 - Th_2 switch in MAP infection

The immune response towards a Mycobacterium avium ssp. paratuberculosis (MAP) infection in ruminants is usually characterized by a initially strong Th_1 response that regresses in the course of infection and is displaced by a Th_2 response as the disease reaches clinical stage [23]. In [22] a mathematical model is proposed to investigate different mechanisms that possibly lead to this switch without taking into account the cross-inhibition of Th_1 and Th_2 cells. The model consists of six nonlinear differential equations each describing the temporal behavior of one of the six variables considered in the model: The concentration of naive CD 4 T cell, T_{h_0}, Th_1 and Th_2 cells, T_{h_1}, T_{h_2}, macrophages, M_Φ, infected macrophages, I_m and free i.e. extracellular bacteria B. The interactions of these populations assumed in the model are shown in Figure 3.4.

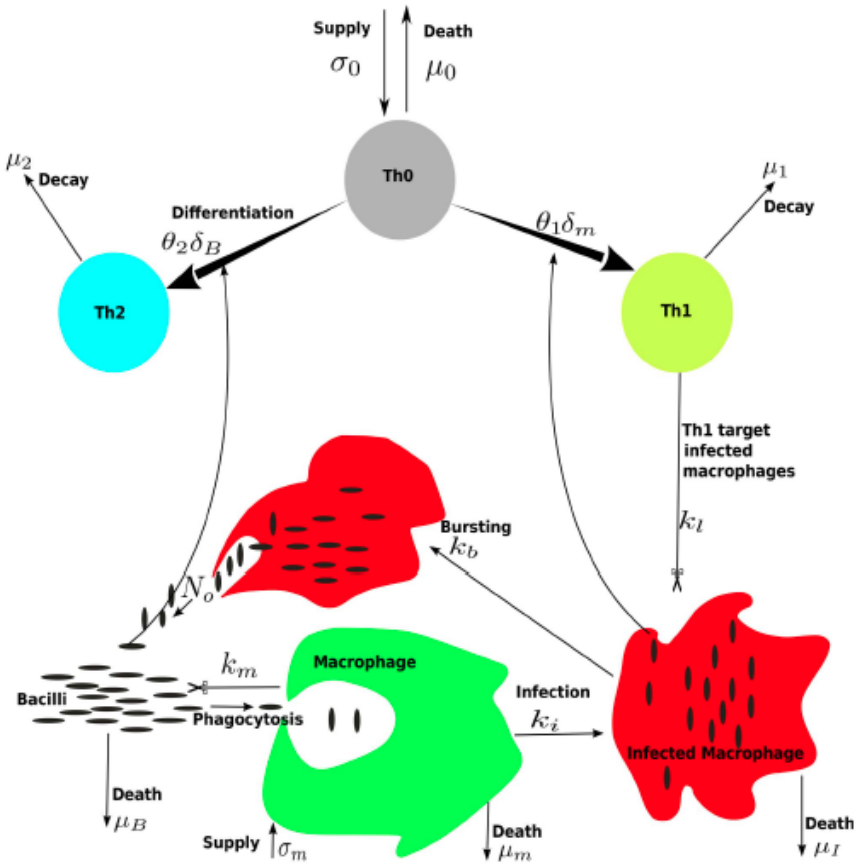

Figure 3.4: Interactions described in (3.5) [22]

In words, the assumptions in this model are the following: naive CD4 T cells are produced at a rate σ_Φ and die at a rate μ_0. They differentiate into Th_1 and Th_2 cells at per capita rates δ_m and δ_B respectively, where differentiation into Th_1 cells depends on the concentration of infected macrophages while differentiation into Th_2 cells is driven by free bacteria. Furthermore one naive CD4 T cell primes into Θ_1 Th_1 or into Θ_2 Th_2 cells. The respective decay rates of Th_1 and Th_2 cells are μ_1 and μ_2. Macrophages are recruited from the blood to the site of infection at a rate σ_m [22] and die at rate μ_m. They phagocytize bacteria at rate k_m thereby becoming infected at a rate k_i. Infected macrophages either get cleared by targeting Th_1 cells which happens at rate k_l or burst thereby producing N_0 new free bacteria. The death rate of infected macrophages is μ_I the one of extracellular bacteria μ_B. All the interactions in this model are density dependent which leads to the following

equations:

$$\begin{aligned}
\frac{dM_\Phi}{dt} &= \sigma_\Phi - k_i M_\Phi B - \mu_m M_\Phi, \\
\frac{dI_m}{dt} &= k_i M_\Phi B - k_b I_m - k_l I_m T_{h_1} - \mu_I I_m, \\
\frac{dB}{dt} &= N_0 k_b I_m - k_i M_\Phi B - k_m M_\Phi B - k_m M_\Phi B - \mu_B B, \\
\frac{dT_{h_0}}{dt} &= \sigma_0 - (\delta_m I_m + \delta_B B) T_{h_0} - \mu_0 T_{h_0}, \\
\frac{dT_{h_1}}{dt} &= \Theta_1 \delta_m I_m T_{h_0} - \mu_1 T_{h_1}, \\
\frac{dT_{h_2}}{dt} &= \Theta_2 \delta_B B T_{h_0} - \mu_2 T_{h_2}.
\end{aligned} \tag{3.5}$$

In experiments, four different patterns in the dynamics of Th_1 and Th_2 immune response during an MAP infection have been observed. First, an initially strong cellular immune response that starts regressing and extinguishes over time. While the cellular immune response decreases, the humoral immune response grows stronger. Second, a delayed switch from Th_1 to Th_2 response is observed. Third, both types of immune response coexist and fourth, the cellular immune response is dominant all the time and hardly any humoral response can be recognized.

The model was used to predict the dynamical interactions that can explain each of the four patterns. It predicts that if extracellular bacteria are long lived, the switch from Th_1 to Th_2 response can be observed. It further predicts that, by increasing the death rate of extracellular bacteria, i.e. by assuming a shorter life time, the switch can be removed, while still both immune responses take place. Further, by performing sensitivity analysis and data fitting, the authors found that their model can fit all possible patterns of $Th_1 - Th_2$ dynamics and that the parameters with the most influence on the dynamics are the initial bacterial dose and parameters determining the kinetics of the immune response [22], such as the death and differentiation rates of Th_1 and Th_2 cells, the magnitudes of clonal expansion of Th_1 and Th_2 cells, i.e. the numbers of Th_1 or Th_2 cells originating from the same mother cell, and the macrophage infection and burst rates.

We will later introduce a similar model to describe the immune response of cattle following a vaccination against Brucella abortus.

Chapter 4

Understanding the immune responses induced by vaccination against brucella infection

4.1 Introduction

Brucellosis is a big problem in cattle industry. Therefore it is important to know how the spreading of this disease can be prevented. As in many other diseases, vaccination plays an important role in this prevention. There are two different vaccine regimes involving to bacteria strains currently available against Brucella abortus. In [13], a study on different vaccination strategies is conducted involving two cohorts of 20 cows each. The first group was vaccinated using the brucella strain RB51, while the second group was administered strain 19. One year after the primary vaccination, both groups were given a booster with strain RB51. Blood samples were taken at the days 0, 28, 210, 365, 393 and 575 after the primary vaccination. The immune cells and chemicals determined from the blood samples are given in Table 4.1.

The data for the different cell populations, cytokines and chemokines are not all given as concentrations but in various different units. The cell populations are given in percentages above or below baseline. Some of the cytokines and chemokines are given as concentrations. For others the magnitude of expansion is measured. Moreover, for several cows considered in the studies we have missing data. There are some cows for which we do not have any data after a certain time. A subset of these cows died during the study, while for other cows, there are other reasons for not having gained any data at certain times.

One of our interests is to compare the immune reactions for the two different vaccine strategies. In this section we aim to determine whether we can find any significant differences of the percentage of cows that respond in a positive manner depending on the vaccination strategy applied. We develop a system of distributing points depending on the performance

of a particular component of the immune system. The final score of an individual cow indicates how good it performs from the point of view of its immune response to the vaccine.

4.2 Measure of immune response

Let $X_j(t), j = 1, \ldots, 23$, be the 23 different variables measured following vaccination. The order of the variables is as in Table 4.1. Time points $t \in \{0, 28, 210, 365, 393, 575\}$ are the days after vaccination when blood samples are taken. For $j = 1, \ldots, 23$ and $t \in \{0, 28, 210, 365, 393, 575\}$ we compute the arithmetic mean $\overline{X}_{j,t}$ and the standard deviation $\sigma(X_{j,t})$ of the entire population. Missing data are removed in these calculations.

Not all the factors for which we have data are equally important in building up protection against brucellosis. Some are preventing the success of the vaccination whereas others indicate that protection is being built up. Due to contradictory reports regarding the roles of some cell types in an immune response, there are factors whose influence on the immune response is not entirely understood yet. Based on discussions with Dr. Dorneles, Dr. Lage and Dr. Sriranganathan, we assign to each factor considered in the blood samples a weight, representing the factor's influence and importance in the immune responses. Table 4.1 shows a list of the factors and their corresponding weights given on a scale from 1 to 10. Factors whose role is unknown are assigned the weight 0, positive factors have positive weights and negative factors negative weights. We did not obtain any information for CD21 memory T cells. Since CD4 memory T cells as well as CD8 memory T cells were assigned the weight 10 we decided to assign the same weight to CD21 memory T cells.

Table 4.1: Weights of factors used in statistical analysis

Positive Factors	Description	Weight
IFN-γ	IFN-γ production	10
CD4-IFN-γ	IFN-γ producing CD4 T cells	10
CD8-GranzymeB	GranzymeB producing cytotoxic CD8 T cells	10
CD8-Perforin	Perforin producing cytotoxic CD8 T cells	10
CD4-CD45R0	CD4 memory T cells	10
CD8-CD45R0	CD8 memory T cells	10
CD21-CD45R0	CD21 memory T cells	10
CD4 Proliferation		9
CD8 Proliferation		9
IL-6	IL-6 production	7
CD8-IFN-γ	IFN-γ producing CD8 T cells	7
MIF CD4-MHCII	Median of intensity of flourescence of MHC class II in CD4 T cells	7
Negative Factors		
CD4-IL-4	IL-4 producing CD4 T cells	-10
IL-4	IL-4 production	-10
CD8-IL-4	IL-4 producing CD8 T cells	-8
CD21-IL-4	IL-4 producing CD21 T cells	-8
IL-10	IL-10 expression	-7
TGF-β	TGF-β expression	-7
Unknown factors		
CD4-FoxP3-CD25High	Regulatory CD4 T cells producing high amounts of IL-10	0
CD4-FoxP3-CD25Low	Regulatory CD4 T cells producing low amounts of IL-10	0
CD8-CD25High	Activated CD8 T cells	0
CD4-IL-17A	IL-17 producing CD4 T cells	0
CD8-IL-17A	IL-17 producing CD8 T cells	0

Referring to Table 4.1 we define a vector w of weights where w_j is the weight belonging to factor X_j.

$$w = (10, 10, 10, 10, 10, 10, 10, 9, 9, 7, 7, 7, -10, -10, -8, -8, -7, -7, 0, 0, 0, 0, 0) \tag{4.1}$$

Next, we describe an algorithm to distribute points to each cow in each cohort, such that a high final score of a single cow indicates a good response, i.e. probably protection against brucella infection. Contrarily a low final score indicates weak protection against subsequent brucella infection. For factors that are assigned positive weights in Table 4.1, high values have positive impact on building up protection, whereas for negative factors low values have a positive effect on protection.

Let $K = \{1, \ldots, 20\}$, $J = \{1, \ldots, 23\}$ and $T = \{0, 28, 210, 365, 393, 575\}$. Then $X_{j,t,k}$, where $j \in J, t \in T$ and $k \in K$, is the measurement of factor j at time t obtained from cow k. $\overline{X}_{j,t}$ is the arithmetic mean of factor X_j over the entire cohort at time t and $\sigma(X_{j,t})$ is the corresponding standard deviation. We say that the value of some measurement $X_{j,t,k}$ is high when it is above the mean $\overline{X}_{j,t}$ of the entire cohort, i.e. $X_{j,t,k} > \overline{X}_{j,t}$, and low when $X_{j,t,k} < \overline{X}_{j,t}$.

Definition 6. *Let K, J and T as above. For $j \in J$, $t \in T$ and $k \in K$ define $p_{j,t,k}$ by the*

difference between $X_{j,t,k}$ and $\overline{X}_{j,t}$, in the following way:

$$p_{j,t,k} = sign(X_{j,t,k} - \overline{X}_{j,t}) \left\lfloor \frac{|X_{j,t,k} - \overline{X}_{j,t}|}{\frac{1}{4}\sigma\left(X_{j,t}\right)} \right\rfloor .$$

The final score of cow k is defined as

$$C_k = \sum_{j\in J} \sum_{t\in T} p_{j,t,k} w_j = \sum_{j\in J} \sum_{t\in T} sign(X_{j,t,k} - \overline{X}_{j,t}) \left\lfloor \frac{|X_{j,t,k} - \overline{X}_{j,t}|}{\frac{1}{4}\sigma\left(X_{j,t}\right)} \right\rfloor w_j \tag{4.2}$$

Nonavailable data are ignored in this summation. The normalization by the standard deviation in the expression of $p_{j,t,k}$ is performed to account for the different units in our variables. The quarter factor was chosen arbitrarily.

4.3 Results and Discussion

Based on (4.2) we assume that the immune response of a cow with a high (positive) final score is more likely to correspond to protection against brucellosis compared to the one of a cow with a low (negative) final score. We say a cow with a positive final score is a good responder whereas a cow with a negative final score is a bad responder. If for one cow there are not any or hardly any data after some point in time we exclude it from our investigations. In the case of the RB51 vaccine we excluded cows $\{2, 3, 4, 5, 8, 11, 16, 18, 20\}$.

Table 4.2: Final scores for strain RB51 as initial vaccine

C1	C2	C3	C4	C5	C6	C7	C8	C9	C10
539	324	164	218	27	741	933	-322	142	-338
C11	C12	C13	C14	C15	C16	C17	C18	C19	C20
22	-802	270	-74	-771	-359	-177	24	-197	-31

According to Table 4.2 we have five good and six bad responders. This corresponds to percentages of 45% (55%) cows that are protected (unprotected) following vaccination. After excluding cow 6 and 17 from the strain 19 dataset we obtain the same percentages as in the case of first vaccinating with RB51.

Table 4.3: Final scores for strain 19 as initial vaccine

C1	C2	C3	C4	C5	C6	C7	C8	C9	C10
528	211	144	-913	-71	-97	-382	-1	524	-277
C11	C12	C13	C14	C15	C16	C17	C18	C19	C20
-125	388	1259	-402	431	-305	-299	108	-384	-311

Comparing the percentages obtained from Table 4.2 and Table 4.3 we do not see any significant difference in the amount of good responders versus bad responders between the two vaccine strategies. One problem in these considerations is certainly the small sample size of only eleven cows in the RB51 set.

We are also interested to see how these percentages change when we only take into account the positive i.e. protection building components of the cellular immune response. These are all positive factors in Table 4.1 with the exception of IFN-γ, IL-6 and MIF CD4-MHCII. The scores for strain RB51 and strain 19 can be seen in Tables 4.4 and 4.5, respectively.

Table 4.4: Final scores for strain RB51 not considering cytokines and negative factors

C1	C2	C3	C4	C5	C6	C7	C8	C9	C10
223	-65	72	130	-33	363	850	-306	-83	114
C11	C12	C13	C14	C15	C16	C17	C18	C19	C20
99	-303	202	-198	-87	-71	-164	-97	-164	-19

The percentages associated with these scores after excluding cows with not enough available data are 45% good responders versus 55% bad responders when the first vaccine given is the RB51 strain and 55% good responders versus 45% bad responders when first vaccinating with strain 19. This shows that the components of the immune response which are responsible for building up protection against brucellosis seem to do so in about 10% more of the cases when first vaccinating with strain 19 compared to first giving the vaccine strain RB51.

Table 4.5: Final scores for strain 19 not considering cytokines and negative factors

C1	C2	C3	C4	C5	C6	C7	C8	C9	C10
294	149	159	-613	-11	-154	-576	19	185	-284
C11	C12	C13	C14	C15	C16	C17	C18	C19	C20
-26	133	1024	-230	495	-233	-200	103	-175	151

4.4 Cluster Analysis

In order to gain a deeper understanding of the data we determine the similarities among cows in the same cohort. The scores described in 4.2 only inform us about whether a cow is a good or bad responder over all. Similar scores for two cows are not necessarily an indicator for similar immune responses, since they can loose and gain their points for performances of distinct factors. We will now define a function measuring the difference in the performances of two cows. Before being able to define the function we first need to rescale the data, since in the original dataset different factors have different units.

Definition 7. *Let* $i \in I = \{1, \ldots, 23\}$, $k \in K = \{1, \ldots, 20\}$, $t \in T = \{0, 28, 210, 365, 393, 575\}$ *and* $X_{i,k,t}$ *be the value of factor* i *of cow* k *measured at time* t. *Let further*

$$X_{i,t}^{+} = \max_{k} X_{i,k,t}$$

and

$$X_{i,t}^{-} = \min_{k} X_{i,k,t}$$

We scale $X_{i,k,t}$ *by setting*

$$\widetilde{X}_{i,k,t} = \frac{X_{i,k,t} - X_{i,t}^{-}}{X_{i,t}^{+} - X_{i,t}^{-}}.$$

Using the last definition we see that all values $\widetilde{X}_{i,k,t}$ are in the range $[0, 1]$. We can now define a function measuring the distance between the performance of two cows in the same cohort in the following way.

Definition 8. *Let* $i \in I, k \in K, t \in T$ *and* $\widetilde{X}_{i,k,t}$ *as in definition 7. Let* C_k *be cow* k. *Then a function dist measuring the differnce in the performance of cow* m *and cow* n *is given by*

$$dist(C_m, C_n) = \frac{1}{p} \sum_{t \in T} \sum_{i \in I} \left| \widetilde{X}_{i,m,t} - \widetilde{X}_{i,n,t} \right|, \qquad m, n \in \{1, \ldots, 20\}$$

where p *is the number of summations. This number differs since we ignore any summand for which at least one of the measurements* $\widetilde{X}_{i,m,t}$ *or* $\widetilde{X}_{i,n,t}$ *is missing.*

The function *dist* is defined such that the smaller the value of $dist(C_m, C_n)$, the more similar the immune reactions are between cow m and cow n. Furthermore, *dist* is symmetric, i.e. $dist(C_m, C_n) = dist(C_n, C_m)$, which is a direct consequence from the symmertry of the absolute value.

Next, we group the cows into clusters using the complete-linkage method implemented in the 'stats' package [27] in R [28]. In the beginning each cow is its own cluster. The distance between two clusters is defined as the furthest distance between any two cows in distinct clusters. In every step the two clusters with the smallest distance are merged. This is repeated until all clusters have been merged into a single cluster. In our cluster analysis we only consider cows for which we have reasonably many data. We define that reasonably many data are given for one cow if there are measurements for at least 12 out of 23 different factors at each time and each factor is measured at least 4 out of 6 times. The cluster tree obtained for the data when first vaccinating with strain RB51 or strain 19 are given in Figures 4.1 and 4.2, respectively.

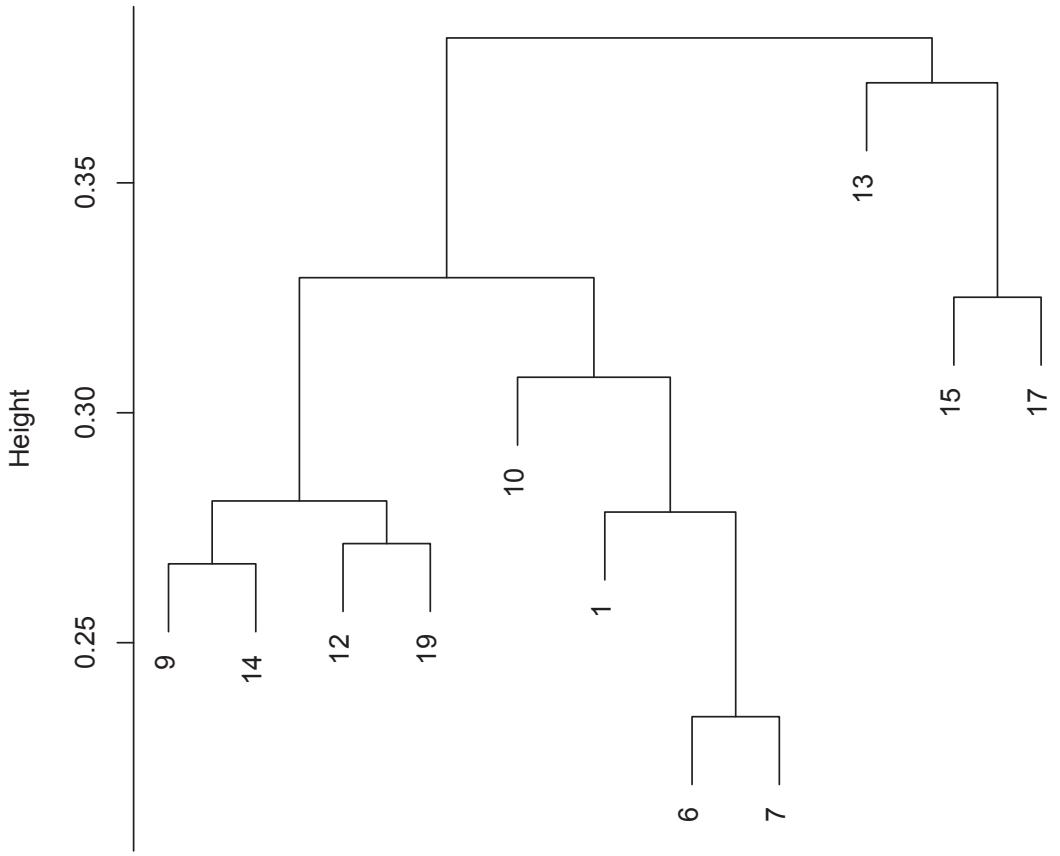

Figure 4.1: Cluster tree for RB51 dataset

Cows 6 and 7 are performing in the most similar manner. Together with the results from Tables 4.2 and 4.4 this leads to the assumption that these two cows are good responders that show similar immune reactions. Another set of cows that cluster together are cows 9, 14, 12 and 19. In contrast to cow 6 and 7 their scores, as given by (4.2) and Tables 4.2 and 4.4, do not necessarily indicate a protection building immune response. Even though cow 9 does have a positive score in the first scoring, we assume it to be a representative for the bad performing set, since its reaction is similar to the one of cow 14, 12 and 19. Having these results we now investigate if we can find factors where the performance of good performers such as cow 6 and 7 significantly differs from the performance of bad performers such as 9, 12, 14 and 19. We are in particular interested if we can see any differences in the Th_1 or Th_2 response to the vaccination. For that we develop a dynamical model for the differences in the reactions of the two cow cohorts when performing homologous prime-boost immunization with two administrations of strain RB51 or heterologous prime-boost vaccination with one administration of strain 19 followed by an administration of strain RB51.

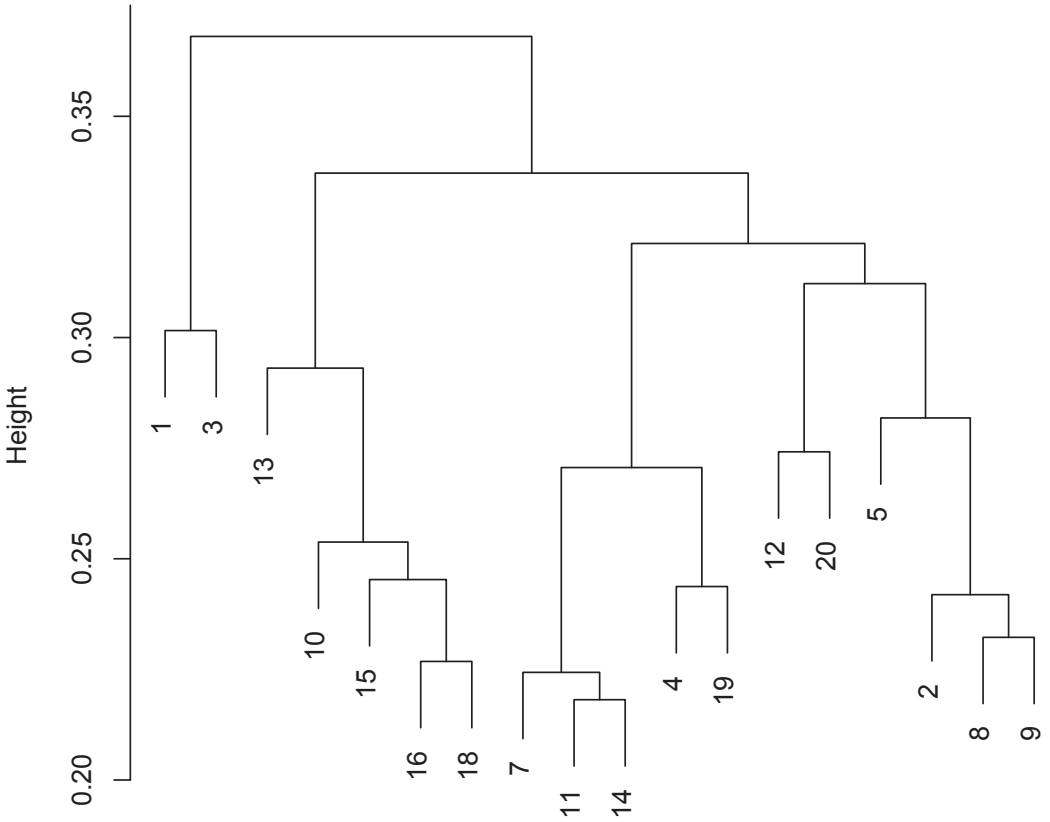

Figure 4.2: Cluster tree for S19 dataset

Chapter 5

Modeling memory CD4 T cell formation following vaccination against brucella infection

5.1 Introduction

Of all the variables, memory CD4 T cells are the only markers that give a consistent difference in behavior between the two cohorts. We next investigate their dynamics.

Computing the arithmetic mean of the memory CD4 T cells at each time point for both cohorts and comparing the time evolution of these means reveals different behavior in the cohort that was first vaccinated with strain RB51 and boostered with strain RB51 (see Figure 5.1) compared to the one first vaccinated with strain 19 and then boostered with strain RB51 (see Figure 5.2). Following primary vaccination with strain RB51 there is an initial rise of memory CD4 T cells followed by a decrease back to the original value within the first year after the primary vaccination. The booster with strain RB51 leads again to a rise in memory CD4 T cells. The peak of cells observed four weeks after the booster is approximately 1.7 times as high as the peak observed four weeks after vaccination. Within the first 210 days after the booster the population size of memory CD4 T cells is nearly back to its original size.

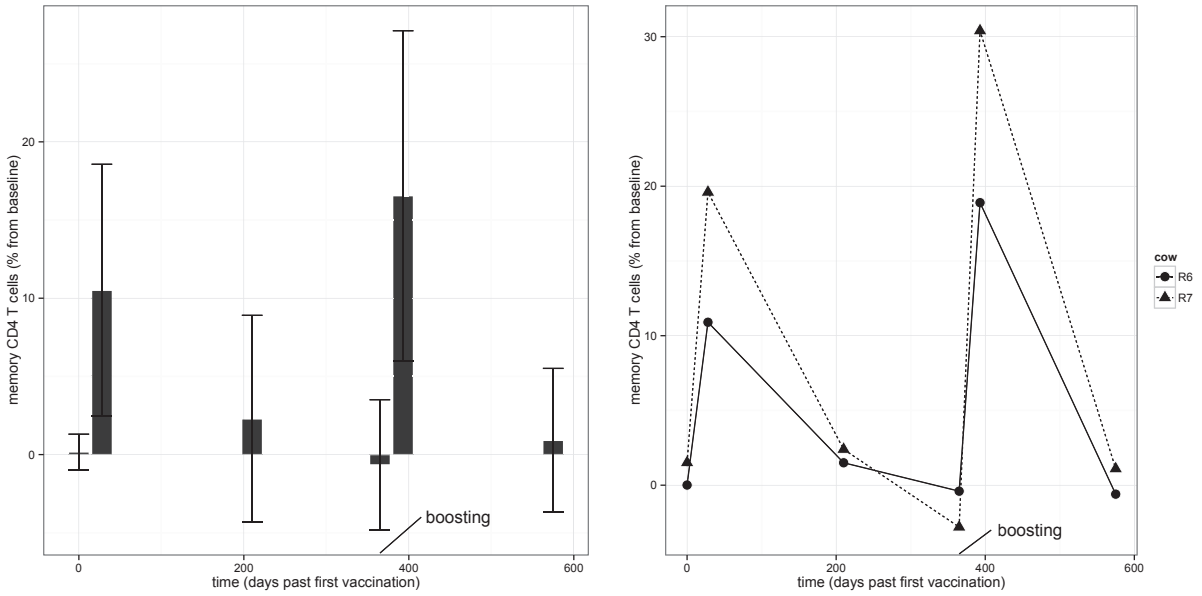

Figure 5.1: Mean value and SD of memory CD4 T cells among 20 cows in RB51 cohort (left panel) together with the values for cows 6 and 7 (right panel) over time

For the cows where strain 19 was used as the initial vaccine, the initial increase in memory CD4 T cells is similar to the one observed when the primary vaccine is strain RB51. Differences occur during the following months. Within the first year following vaccination with strain 19, the mean population of memory CD4 T cells levels off to a positive value significantly greater than its initial size (see Figure 5.2). Four weeks after boosting with strain RB51, we observe a significant rise in the amount of memory CD4 T cells. This is followed by a leveling off within the next months to approximately the same equilibrium value seen before the booster.

The differences in the memory cell dynamics among the two vaccination regimes has led us to assume that the increased pool of memory CD4 T cells persisting after the booster originates in the primary vaccination with strain 19.

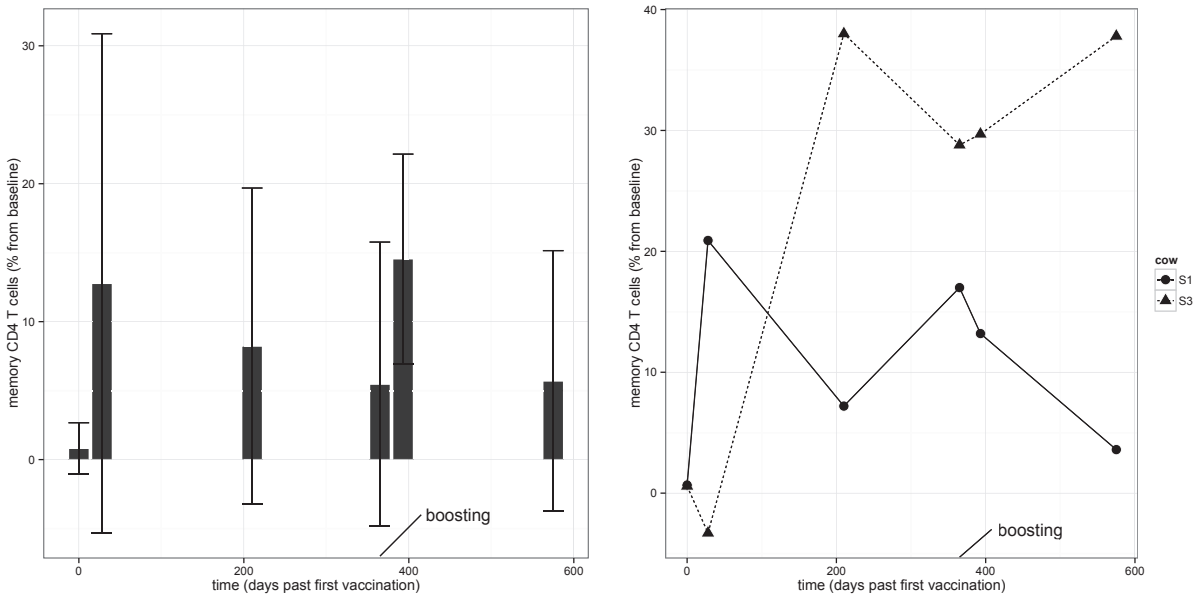

Figure 5.2: Mean value and SD of memory CD4 T cells among 20 cows in S19 cohort (left panel) together with the values for cows 1 and 3 (right panel) over time

In the following sections we introduce a mathematical model for the dynamics of different CD4 T cell subpopulations following a vaccination, with a focus on the dynamics of memory CD4 T cells. We want to use that model to determine the factors that lead to the loss of memory cells in one case and to persistence in another.

5.2 Model Development

We develop a model that describes the interaction between antigen-specific naive CD4 T cells, N, two types of effector CD4 T cells, Th_1 and Th_2, antigen presenting activated macrophages, Φ, and memory CD4 T cells, M in the following way. The immune response is initiated by administering the vaccine which is represented in a high amount of activated macrophages Φ_0. We assume that macrophages are supplied from progenitor monocytes that are recruited from the blood [22] and activated by Th_1 cells at a rate σ_Φ. They decay at per capita rate d_Φ. Naive CD4 T cells differentiate into effector CD4 T cells Th_1 and Th_2 at per capita rates δ_1 and δ_2, respectively. We make the assumption that the differentiation of naive CD4 T cells into Th_1 cells depends on the density of activated macrophages while the differentiation of naive CD4 T cells into Th_2 cells does not. In our model these relations are displayed in the production terms $\delta_1\Theta_1 N\Phi$ and $\delta_2\Theta_2 N$ for Th_1 and Th_2 effector cells. $\Theta_1 \gg 0$ and $\Theta_2 \gg 0$ are parameters determining the magnitude of clonal expansion of the Th_1 and Th_2 responses, respectively [22]. Effector CD4 T cells Th_1 and Th_2 die at per

capita rates d_1, d_2 and differentiate into memory CD4 T cells at per capita rates m_1 and m_2, respectively. Naive CD4 T cells are produced by the thymus [8] at a constant rate σ_N and die at per capita rate d_N. The survival of memory CD4 T cells depends on the availability of the cytokine IL-7. This leads to a limited carrying capacity K for memory CD4 T cells [18]. Since all CD4 T cells use this cytokine [20] we assume competition between memory and effector CD4 T cells. This competition is expressed in our model by the term

$$mM\left(1-\frac{\alpha_M M+\alpha_1 Th_1+\alpha_2 Th_2}{K}\right),$$

where α_1, α_2 and α_M are scaling parameters that indicate how much of the memory CD4 T cells' environment is used by Th_1 and Th_2 cells, respectiveley.

The system of equations describing these interactions is given in (5.1) and a schematic representation is shown in Figure 5.3.

$$\begin{aligned}
\frac{dN}{dt} &= \sigma_N-\delta_1\Phi N-\delta_2 N-d_N N,\\
\frac{dTh_1}{dt} &= \delta_1\Theta_1\Phi N-d_1 Th_1-m_1 Th_1,\\
\frac{dTh_2}{dt} &= \delta_2\Theta_2 N-d_2 Th_2-m_2 Th_2,\\
\frac{d\Phi}{dt} &= \sigma_\Phi Th_1-d_\Phi\Phi,\\
\frac{dM}{dt} &= m_1 Th_1+m_2 Th_2+mM\left(1-\frac{\alpha_1 Th_1+\alpha_2 Th_2+\alpha_M M}{K}\right).
\end{aligned} \tag{5.1}$$

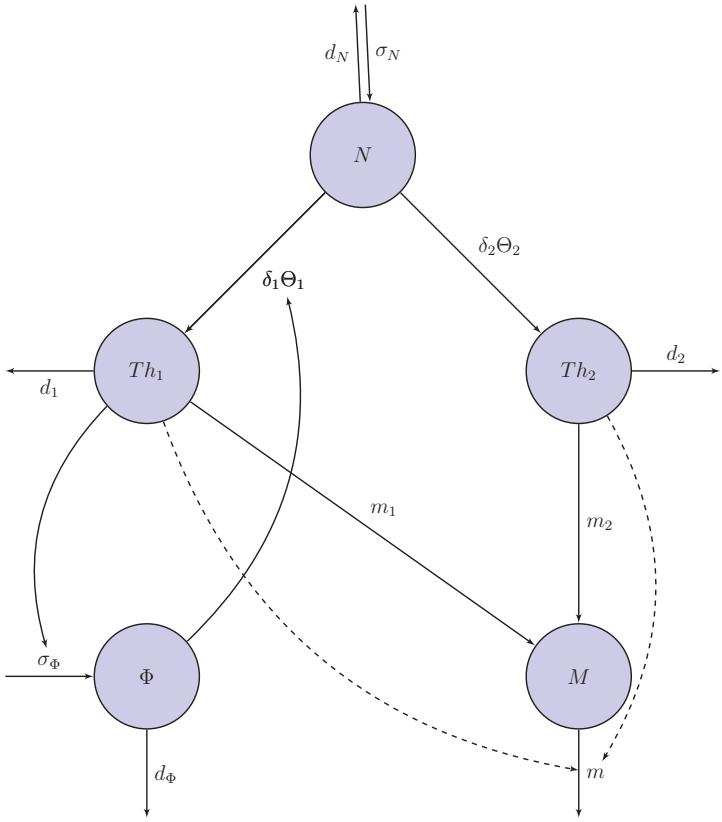

Figure 5.3: Diagram for the model (5.1)

5.3 Analytical Results

5.3.1 Positivity and Boundedness

Our goal in this section is to establish the positivity and boundedness of the initial value problem (5.1) with initial values

$$\begin{aligned} &N(0) = N_0 > 0, Th_1(0) = Th_{10} > 0, Th_2(0) = Th_{20} > 0, \\ &\Phi(0) = \Phi_0 > 0, M(0) = M_0 > 0. \end{aligned} \tag{5.2}$$

Lemma 4. *There is a maximal $b > 0$ such that the initial value problem (5.1) subject to initial conditions (5.2) has a unique solution on $[0, b)$. This solution is positive on $[0, b)$.*

Proof. Let $y(t) = [N(t), Th_1(t), Th_2(t), \Phi(t), M(t)]^T$ and $f : D \subset \mathbb{R}^5 \to \mathbb{R}^5$ with

$$f(t,y) = \begin{pmatrix} \sigma_N - \delta_1 \Phi N - \delta_2 N - d_N N \\ \delta_1 \Theta_1 \Phi N - d_1 Th_1 - m_1 Th_1 \\ \delta_2 \Theta_2 N - d_2 Th_2 - m_2 Th_2 \\ \sigma_\Phi Th_1 - d_\Phi \Phi \\ m_1 Th_1 + m_2 Th_2 + mM\left(1 - \frac{\alpha_1 Th_1 + \alpha_2 Th_2 + \alpha_M M}{K}\right) \end{pmatrix}. \tag{5.3}$$

Then the initial value problem (5.1) subject to initial conditions (5.2) is equivalent to

$$y'(t) = f(t, y(t)),\ y(0) = [N_0, Th_{10}, Th_{20}, \Phi_0, M_0]^T. \tag{5.4}$$

Since f and $\dfrac{\partial f}{\partial y}$ are continuous in y, the conditions of Lemma 1 are satisfied. Then by Lemma 1 there exists a maximal value $b > 0$ such that (5.4) has a unique solution on the interval $[0, b)$.
Let $t_1 \in (0, b)$ and assume that all variables are positive on $[0, t_1)$. Then, due to continuity, all variables are non-negative on the interval $[0, t_1]$. Therefore for $t \in [0, t_1]$

$$\begin{aligned} \frac{dTh_1}{dt}(t) &= \delta_1 \Theta_1 \Phi(t) N(t) - d_1 Th_1(t) - m_1 Th_1(t) \\ &\geq -(d_1 + m_1) Th_1(t). \end{aligned}$$

This implies $Th_1(t_1) \geq Th_{10} e^{-(d_1+m_1)t_1} > 0$. Hence, we know that if all the variables are positive on $[0, t_1)$ then Th_1 is positive on $[0, t_1]$. Using similar arguments we obtain that if all variables are positive on $[0, t_1)$ then Φ and Th_2 are positive on $[0, t_1]$.
Since Φ is continuous, it is bounded on the compact set $[0, t_1]$. Thus, there is a constant C_1 such that $\Phi(t) \leq C_1$ for all $t \in [0, t_1]$. Therefore

$$\begin{aligned} \frac{dN}{dt}(t) &= \sigma_N - \delta_1 \Phi(t) N(t) - \delta_2 N(t) - d_N N(t) \\ &\geq -(\delta_1 C_1 + \delta_2 + d_N) N(t). \end{aligned}$$

which implies $N(t_1) \geq N_0 e^{-(\delta_1 C_1 + \delta_2 + d_N)t_1} > 0$. I.e. if all variables are positive on $[0, t_1)$, then the positivity of N extends to $[0, t_1]$.
The continuity of Th_1, Th_2 and M implies their boundedness on the compact interval $[0, t_1]$. Thus, there exists a constant C_2 such that $\dfrac{\alpha_1 Th_1 + \alpha_2 Th_2 + \alpha_M M}{K} \leq C_2$ on $[0, t_1]$. Combined with the positivity of Th_1 and Th_2 on $[0, t_1]$ we can estimate for $t \in [0, t_1]$

$$\begin{aligned} \frac{dM}{dt}(t) &= m_1 Th_1(t) + m_2 Th_2(t) + mM(t)\left(1 - \frac{\alpha_1 Th_1(t) + \alpha_2 Th_2(t) + \alpha_M M(t)}{K}\right) \\ &\geq mM(t)(1 - C_2). \end{aligned}$$

Hence $M(t_1) \geq M_0 e^{(1-C_2)t_1} > 0$.
Concluding all the results we got so far, we know that under the assumption that all variables

are positive on $[0, t_1)$ they are also positive on $[0, t_1]$. Assume the solution y is not positive on $[0, b)$. Then due to the continuity of the solution, there is a smallest $t_2 \in (0, b)$ such that y is positive on $[0, t_2)$ but not on $[0, t_2]$. Since in above reasoning $t_1 \in (0, b)$ is chosen arbitrarily, we know that y positive on $[0, t_2)$ implies y positive on $[0, t_2]$, a contradiction. This finishes the proof. □

Lemma 5. *The solution of (5.1) subject to initial condition (5.2) found in Lemma 4 is bounded on* $[0, b)$.

Proof. Let $G(t) = \Theta_1 N(t) + Th_1(t)$ and $C_1 = \min\{\delta_2 + d_N, d_1 + m_1\}$. Then for t in $[0, b)$

$$\begin{aligned}\frac{dG}{dt}(t) &= \Theta_1\sigma_N - \Theta_1 N(t)(\delta_2 + d_N) - Th_1(t)(d_1 + m_1)\\ &\leq \Theta_1\sigma_N - C_1\left(\Theta_1 N(t) + Th_1(t)\right)\\ &= \Theta_1\sigma_N - C_1 G(t),\end{aligned}$$

which implies $G(t) \leq \max\left\{G(0), \frac{\Theta_1\sigma_N}{c_1}\right\} = C_2$ for $t \in [0, b)$. Since N and Th_1 are positive on $[0, b)$ this implies $N(t) \leq C_2$ and $Th_1(t) \leq C_2$ for $t \in [0, b)$. Thus N and Th_1 are bounded on $[0, b)$.
Since N is bounded on $[0, b)$, there is a constant $C_3 > 0$ such that $\delta_2\Theta_2 N(t) < C_3$ for $t \in [0, b)$. Therefore for $t \in [0, b)$

$$\begin{aligned}\frac{dTh_2}{dt} &= \delta_2\Theta_2 N - d_2 Th_2 - m_2 Th_2\\ &\leq C_3 - (d_2 + m_2)Th_2.\end{aligned}$$

This allows us to estimate $Th_2(t) \leq \max\left\{Th_2(0), \frac{C_3}{d_2 + m_2}\right\}$. Hence Th_2 is bounded on $[0, b)$.
Using similar arguments the boundedness of Th_1 implies the boundedness of Φ on $[0, b)$.
Since Th_1 and Th_2 are bounded on $[0, b)$ there exists a constant $C_4 > 0$ such that $m_1 Th_1 + m_2 Th_2 \leq C_4$ on $[0, b)$. Furthermore, the solution is positive on $[0, b)$ and therefore

$$\frac{\alpha_1 Th_1 + \alpha_2 Th_2 + \alpha_M M}{K} > 0$$

on $[0, b)$. Hence we have

$$\left(1 - \frac{\alpha_1 Th_1 + \alpha_2 Th_2 + \alpha_M M}{K}\right) \leq 1 - \frac{\alpha_M}{K} M$$

and obtain for $t \in [0, b)$

$$\begin{aligned}\frac{dM}{dt} &= m_1 Th_1(t) + m_2 Th_2(t) + mM(t)\left(1 - \frac{\alpha_1 Th_1(t) + \alpha_2 Th_2(t) + \alpha_M M(t)}{K}\right) \\ &\leq C_4 + mM(t)\left(1 - \frac{\alpha_M}{K} M(t)\right) \\ &= C_4 + mM(t) - \frac{\alpha_M m}{K} M^2(t).\end{aligned} \tag{5.5}$$

Let M^* be the greater of the two roots of the right-hand side of inequality (5.5). Then

$$M^* = \frac{K}{2\alpha_M} + \sqrt{\frac{K^2}{4\alpha_M^2} + \frac{KC_4}{\alpha_M m}}.$$

(5.5) implies $M(t) \leq \max\{M_0, M^*\}$. In conclusion we have that all variables are bounded on $[0, b)$. □

Lemma 6. *The initial value problem (5.1) subject to initial conditions (5.2) has a unique solution on* $[0, \infty)$*. This solution is positive and bounded.*

Proof. Lemma 4 and Lemma 5 imply that there exists a maximal $b > 0$ such that (5.1) subject to initial conditions (5.2) has a unique solution on $[0, b)$. Furthermore this solution is positive and bounded. Lemma 1 implies $b = \infty$. □

5.3.2 Steady-states

We find the following four steady-states, given in the form

$$\overline{x} = \left[\overline{N}, \overline{Th}_1, \overline{Th}_2, \overline{\Phi}, \overline{M}\right].$$

$$\begin{aligned}\overline{x}_{1,2} = \Bigg[&\frac{\sigma_N}{\delta_2 + d_N},\ 0,\ \frac{\delta_2 \Theta_2 \sigma_N}{(\delta_2 + d_N)(d_2 + m_2)},\ 0, \\ &-\frac{\alpha_2 \overline{Th}_2 - K}{2\alpha_M} \pm \sqrt{\frac{(\alpha_2 \overline{Th}_2 - K)^2}{4\alpha_M^2} + \frac{K m_2 \overline{Th}_2}{m\alpha_M}}\Bigg], \\ \overline{x}_{3,4} = \Bigg[&\frac{d_\Phi(d_1 + m_1)}{\delta_1 \Theta_1 \sigma_\Phi},\ \frac{\sigma_N \delta_1 \Theta_1 \sigma_\Phi - (\delta_2 + d_N)(d_1 + m_1) d_\Phi}{\delta_1 \sigma_\Phi (d_1 + m_1)},\ \frac{\delta_2 \Theta_2 d_\Phi (d_1 + m_1)}{\delta_1 \Theta_1 \sigma_\Phi (d_2 + m_2)}, \\ &\frac{\sigma_N \delta_1 \Theta_1 \sigma_\Phi - (\delta_2 + d_N)(d_1 + m_1) d_\Phi}{\delta_1 d_\Phi (d_1 + m_1)}, -\frac{\alpha_1 \overline{Th}_1 + \alpha_2 \overline{Th}_2 - K}{2\alpha_M} \\ &\pm \sqrt{\frac{(\alpha_1 \overline{Th}_1 + \alpha_2 \overline{Th}_2 - K)^2}{4\alpha_M^2} + (m_1 \overline{Th}_1 + m_2 \overline{Th}_2)\frac{K}{m\alpha_M}}\Bigg].\end{aligned}$$

In our model we consider population sizes. Therefore we are only interested in non-negative real steady-states.

Lemma 7. *Steady-state $\overline{x}_1$ is non-negative and real.*

Proof. $\overline{x}_1$ non-negative and real follows directly since all parameters are positive. □

Lemma 8. *Steady-state $\overline{x}_3$ is non-negative and real iff*

$$\sigma_N \delta_1 \Theta_1 \sigma_\Phi \geq (\delta_2 + d_N)(d_1 + m_1) d_\Phi.$$

Proof. Entries 2 and 4 are non-negative iff above condition is satisfied. For the other three entries non-negative and real follows directly from the positivity of all parameter values and the non-negativity of entries 2 and 4. □

Lemma 9. *Steady-states $\overline{x}_2$ and $\overline{x}_4$ are not non-negative and real.*

Proof. Note that the fifth entry is always negative. □

Therefore only steady-states $\overline{x}_1$ and $\overline{x}_3$ are of biological interest. Steady-state $\overline{x}_1$ describes a state where Th_1 cells and macrophages are extinct and naive CD4 T cells, Th_2 cells and memory CD4 T cells are at constant positive levels. The second steady-state of interest, $\overline{x_3}$, describes a state where all cell types are at a constant positive level.

5.3.3 Stability Analysis

The Jacobian matrix of system (5.1) is given by

$$J = \begin{pmatrix} -(\delta_1 \Phi + \delta_2 + d_N) & 0 & 0 & -\delta_1 N & 0 \\ \delta_1 \Theta_1 \Phi & -(d_1 + m_1) & 0 & \delta_1 \Theta_1 N & 0 \\ \delta_2 \Theta_2 & 0 & -(d_2 + m_2) & 0 & 0 \\ 0 & \sigma_\Phi & 0 & -d_\Phi & 0 \\ 0 & m_1 - \frac{m\alpha_1 M}{K} & m_2 - \frac{m\alpha_2 M}{K} & 0 & C \end{pmatrix},$$

where

$$C = m\left(1 - \frac{\alpha_1 Th_1 + \alpha_2 Th_2 + \alpha_M M}{K}\right) - \frac{m\alpha_M M}{K}.$$

The corresponding eigenvalues are

$$\lambda_1 = C = m\left(1 - \frac{\alpha_1 Th_1 + \alpha_2 Th_2 + \alpha_M M}{K}\right) - \frac{m\alpha_M M}{K},$$

$$\lambda_2 = -(d_2 + m_2),$$

and solutions of

$$\det(\widetilde{J} - \lambda I_3) = 0, \tag{5.6}$$

where

$$\widetilde{J} = \begin{pmatrix} -(\delta_1\Phi + \delta_2 + d_N) & 0 & -\delta_1 N \\ \delta_1\Theta_1\Phi & -(d_1 + m_1) & \delta_1\Theta_1 N \\ 0 & \sigma_\Phi & -d_\Phi \end{pmatrix}.$$

λ is a solution of (5.6) iff it solves

$$\lambda^3 + K_1\lambda^2 + K_2\lambda + K_3 = 0,$$

where

$$\begin{aligned} K_1 &= d_\Phi + d_1 + m_1 + \delta_1\Phi + \delta_2 + d_N, \\ K_2 &= -\sigma_\Phi\delta_1\Theta_1 N + (d_1 + m_1 + d_\Phi)(d_\Phi + \delta_2 + d_N + \delta_1\Phi) - d_\Phi^2 \\ K_3 &= -\sigma_\Phi\delta_1\Theta_1 N(\delta_2 + d_N) + (\delta_1\Phi + \delta_2 + d_N)(d_1 + m_1) \end{aligned}$$

Since $d_2, m_2 > 0$ we have $\lambda_2 < 0$.

We want to investigate the local stability of steady-states $\overline{x}_1$ and $\overline{x}_3$. Let

$$R_0 = \frac{\sigma_\Phi\Theta_1\sigma_N\delta_1}{d_\Phi(d_1 + m_1)(\delta_2 + d_N)}.$$

Lemma 10. *Steady-state $\overline{x}_1$ is locally asymptotically stable iff*

$$R_0 < 1.$$

Proof. In order for any steady-state to be locally asymptotically stable all eigenvalues need to have negative real part. λ_1 has negative real part when

$$0 < 2\Re\left(\sqrt{\frac{(\alpha_2\overline{Th}_2 - K)^2}{4\alpha_M^2} + m_2\overline{Th}_2\frac{K}{m}}\right).$$

This holds since the steady-state Th_2 population size

$$\overline{Th}_2 = \frac{\delta_2\Theta_2\sigma_N}{(\delta_2 + d_N)(d_2 + m_2)}$$

is positive and therefore the square root is some real positive number.
Evaluating $\widetilde{J}$ at the steady-state $\overline{x}_1$ gives us

$$\widetilde{J}|_{\overline{x}_1} = \begin{pmatrix} -(\delta_2 + d_N) & 0 & -\frac{\delta_1\sigma_N}{\delta_2 + d_N} \\ 0 & -(d_1 + m_1) & \frac{\delta_1\Theta_1\sigma_N}{\delta_2 + d_N} \\ 0 & \sigma_\Phi & -d_\Phi \end{pmatrix}.$$

One eigenvalue of $\widetilde{J}|_{\overline{x}_1}$ is $\lambda_3 = -(\delta_2 + d_N)$. Furthermore the remaining two eigenvalues $\lambda_4,\ \lambda_5$ solve the equation $\lambda^2 + K_1\lambda + K_2 = 0$ where

$$\begin{aligned} K_1 &= d_1 + m_1 + d_\Phi, \\ K_2 &= \frac{(d_1 + m_1)(\delta_2 + d_N)d_\Phi - \sigma_N\delta_1\Theta_1\sigma_\Phi}{\delta_2 + d_N}. \end{aligned}$$

Using the Ruth-Hurwitz condition, $\lambda_4,\ \lambda_5$ have negative real part iff

$$K_1 > 0,\ K_1K_2 > 0,$$

which is equivalent to

$$K_1 > 0,\ K_2 > 0.$$

$K_1 > 0$ is satisfied since all parameters are positive. $K_2 > 0$ when $R_0 < 1$. □

Biologically, $R_0 < 1$ implies that when the macrophages and Th_1 decay rates are large compared to their mutual activation rates, then both populations will go extinct. The next result shows that if the inverse is true, i.e. the strength of the mutual activation dominates the decay of macrophages and Th_1 cells, then all cell populations will coexists in the long run.

Lemma 11. *Steady-state $\overline{x}_3$ is locally asymptotically stable iff*

$$R_0 > 1.$$

Proof. Evaluating $\widetilde{J}$ at the steady-state $\overline{x}_3$ yields

$$\widetilde{J}|_{\overline{x}_3} = \begin{pmatrix} -\left(\frac{\sigma_N\delta_1\Theta_1\sigma_\Phi - (\delta_2+d_N)(d_1+m_1)d_\Phi}{d_\Phi(d_1+m_1)} + \delta_2 + d_N\right) & 0 & -\frac{d_\Phi(d_1+m_1)}{\Theta_1\sigma_\Phi} \\ \Theta_1\frac{\sigma_N\delta_1\Theta_1\sigma_\Phi - (\delta_2+d_N)(d_1+m_1)d_\Phi}{d_\Phi(d_1+m_1)} & -(d_1+m_1) & \frac{d_\Phi(d_1+m_1)}{\sigma_\Phi} \\ 0 & \sigma_\Phi & -d_\Phi \end{pmatrix}.$$

Thus the remaining three eigenvalues $\lambda_3,\ \lambda_4,\ \lambda_5$ solve the equation $\lambda^3 + K_1\lambda^2 + K_2\lambda + K_3 = 0$ where

$$\begin{aligned} K_1 &= \frac{d_\Phi^2(d_1+m_1) + d_\Phi(d_1+m_1)^2 + \sigma_N\delta_1\Theta_1\sigma_\Phi}{d_\Phi(d_1+m_1)}, \\ K_2 &= \frac{\sigma_N\Theta_1\sigma_\Phi\delta_1(d_\Phi + d_1 + m_1)}{d_\Phi(d_1+m_1)}, \\ K_3 &= \sigma_N\delta_1\Theta_1\sigma_\Phi - d_\Phi(d_1+m_1)(\delta_2+d_N). \end{aligned}$$

Using the Ruth-Hurwitz condition, $\lambda_3,\ \lambda_4$ and λ_5 have negative real part iff

$$K_1 > 0,\ K_3 > 0 \text{ and } K_1K_2 > K_3.$$

$K_1 > 0$ is always satisfied, $K_3 > 0$ is equivalent to

$$\sigma_N \delta_1 \Theta_1 \sigma_\Phi > d_\Phi (d_1 + m_1)(\delta_2 + d_N)$$

which in turn is equivalent to

$$R_0 > 1.$$

Setting $a = d_\Phi,\ b = (d_1 + m_1),\ c = (\delta_2 + d_N)$ we have $a, b, c > 0$ and

$$\begin{aligned} K_1 &= a + b + cR_0, \\ K_2 &= c(a + b)R_0, \\ K_3 &= abcR_0 - abc. \end{aligned}$$

The condition $K_1 K_2 > K_3$ then yields to the inequality

$$((a + b) + cR_0)R_0 c(a + b) > R_0 abc - abc.$$

This inequality is equivalent to

$$c(a + b)R_0^2 + (a^2 + ab + b^2)R_0 + ab > 0$$

which is satisfied since $a, b, c, R_0 > 0$.
Thus, λ_3, λ_4 and λ_5 have negative real part iff

$$R_0 > 1.$$

Further, λ_2 has negative real part. λ_1 has negative real part iff

$$0 < 2\Re\left(\sqrt{\frac{(\alpha_1 \overline{Th}_1 + \alpha_2 \overline{Th}_2 - K)^2}{4\alpha_M^2} + m_1 \overline{Th}_1 \frac{K}{m} + m_2 \overline{Th}_2 \frac{K}{m}}\right).$$

This holds since

$$\overline{Th}_1 = \frac{\sigma_N \delta_1 \Theta_1 \sigma_\Phi - (\delta_2 + d_N)(d_1 + m_1) d_\Phi}{\delta_1 \sigma_\Phi (d_1 + m_1)}$$

and

$$\overline{Th}_2 = \frac{\delta_2 \Theta_2 d_\Phi (d_1 + m_1)}{\delta_1 \Theta_1 \sigma_\Phi (d_2 + m_2)}$$

are positive iff

$$R_0 > 1.$$

□

5.4 Numerical Results

5.4.1 Parameter Values

In their similar model of immune responses during Mycrobaterium avium paratuberculosis in ruminants Ganusov et al. [22] performed a literature search for their parameters. There is very little quantitative information about immune reactions in cattle to Brucella abortus. We assume that parameters of differentiation or decay of different cell types are independent of the disease and we can use the values from [22]

Initially we assume $N_0 = 0.1$ antigen-specific naive CD4 T cells per ml [22]. They decay at rate $d_N = 0.01$ per day and differentiate into Th_1 and Th_2 cells at per capita rates $\delta_1 = 0.01$ ml per cell per day and $\delta_2 = 0.01$ per day, respectively, and with a magnitude of clonal expansion $\Theta_1 = \Theta_2 = 900$, respectively [22].

Prior to the administration of the vaccine there are no effector CD4 T cells, i.e. $Th_{1_0} = 0$ cells per ml and $Th_{2_0} = 0$ cells per ml. In [22] the decay rate of Th_1 is set to 0.03 per day and the decay rate of Th_2 is set to 0.02 per day. In contrast to the model in [22] we consider memory CD4 T cells. A small percentage of antigen-specific T cells converts into memory cells [20]. Therefore, in our model, we split the parameters of decay into two parameters each: the per capita differentiation rates from effector Th_1 and Th_2 cells into memory CD4 T cells $m_1 = 0.005$ per day and $m_2 = 0.005$ per day, and the decay rates due to other reasons such as death, $d_1 = 0.025$ per day and $d_2 = 0.015$ per day, respectively.

We assume to have an initial concentration of $\Phi_0 = 450$ activated macrophages per ml [22], responsible for the induction of the immune response. Macrophages decay at rate $\sigma_\Phi = 0.02$ per day [22].

Several parameters $\{\sigma_N, \sigma_\Phi, m, K, \alpha_1, \alpha_2, \alpha_M\}$ in our model remain unknown. We use $\sigma_N = 0.01$ cells per ml per day as the constant influx of naive CD4 T cells. The recruitment and activation rate of macrophages by Th_1 cells is $\sigma_\Phi = 0.001$ per day. The maximal growth rate of memory CD4 T cells is set to be $m = 0.01$ per day and for the carrying capacity of memory cells we use $K = 100$ cells per ml. Further we use $\alpha_1 = 1$, $\alpha_2 = 20$ and $\alpha_M = 1$. A summary of all the parameter values is given in Table 5.1.

Table 5.1: Fixed parameter used in simulations

Initial Condition	Description	Value	Unit	Reference
N_0	initial naive CD4 T cells	0.1	cells/ml	[22]
Th_{1_0}	initial Th_1 cells	0	cells/ml	[22]
Th_{2_0}	initial Th_2 cells	0	cells/ml	[22]
Φ_0	initial activated macrophages	450	cells/ml	
M_0	initial CD4 memory cells	0	cells/ml	
Parameter	Description	Value	Unit	Reference
σ_N	constant influx of naive CD4 T cells	0.01	cells/(ml · day)	
σ_Φ	recruitment and activation rate of Φ by Th_1	0.001	per day	
δ_1	per capita differentiation rate N into Th_1 cells	0.01	ml/(cells · day)	[22]
δ_2	per capita differentiation rate N into Th_2 cells	0.01	per (ml · day)	[22]
Θ_1	magnitude of clonal expansion of Th_1 cells	900	-	[22]
Θ_2	magnitude of clonal expansion of Th_2 cells	900	-	[22]
d_N	N decay rate	0.01	per day	[22]
d_1	Th_1 decay rate	0.025	per day	[22]
d_2	Th_2 decay rate	0.015	per day	[22]
d_Φ	decay rate of macrophages	0.02	per day	[22]
m_1	differentiation rate Th_1 into M	0.005	per day	
m_2	differentiation rate Th_2 into M	0.005	per day	
m	maximal growth rate of M	0.01	per day	
K	carrying capacity	100	cells/ml	
α_1	competition of M and Th_1 for cytokines	1	-	
α_2		20	-	
α_M		1	-	

Using the parameters and initial conditions given in Table 5.1 the model's dynamic is simulated in Figure 5.4. The simulated behavior of the memory CD4 T cell population resembles the one we see after the primary vaccination with strain 19 (Figure 5.2). The main characteristics are an initial increase followed by a leveling off to a constant value significantly higher than the initial amount of memory CD4 T cells.

Considering the effector CD4 T cells we see that, in the beginning, the immune response is completely governed by the Th_1-type immune response. Over time there is also a Th_2-type response established but the Th_1-type response remains dominant. The system approaches a steady-state in which all populations coexist ($\overline{x}_3$ locally asymptotically stable).

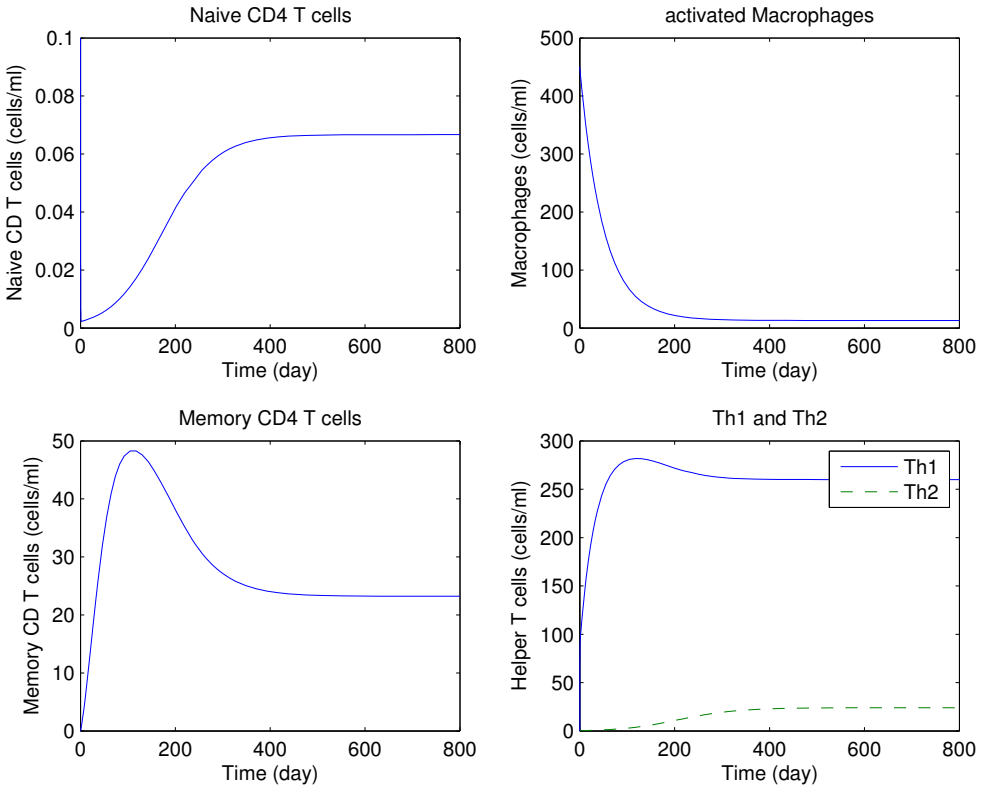

Figure 5.4: Systems dynamics for $\sigma_\Phi = 0.001\text{day}^{-1}$. All other parameters as in Table 5.1.

Decreasing the rate at which Th_1 cells recruit and activate macrophages, σ_Φ, from 0.001 day^{-1} to 0.0001 day^{-1} leads to a change in the dynamics of the system (see Figure 5.5). The system no longer approaches the steady-state in which all cell populations coexist. Instead we now see that after being the predominant type of immune response in the beginning, the Th_1-type immune response completely extinguishes over time while the Th_2-type response overtakes the dominant role. The dynamics of the memory CD4 T cell population can again be characterized by a steep increase in the first few weeks after the vaccination followed by a decline until a steady-state is reached, approximately 13 month after the vaccination. Whereas the peak of the memory CD4 T cell population has approximately the same height as in the coexistence state, the steady-state is noticeably lower. Moreover, in contrast to the coexistence state, the steady-state is similar to the original amount of memory CD4 T cells. Comparing this to the results obtained by evaluating the data gained in experiments, this behavior of memory CD4 T cells is similar to the behavior we find in the first year after giving the strain RB51 vaccine.

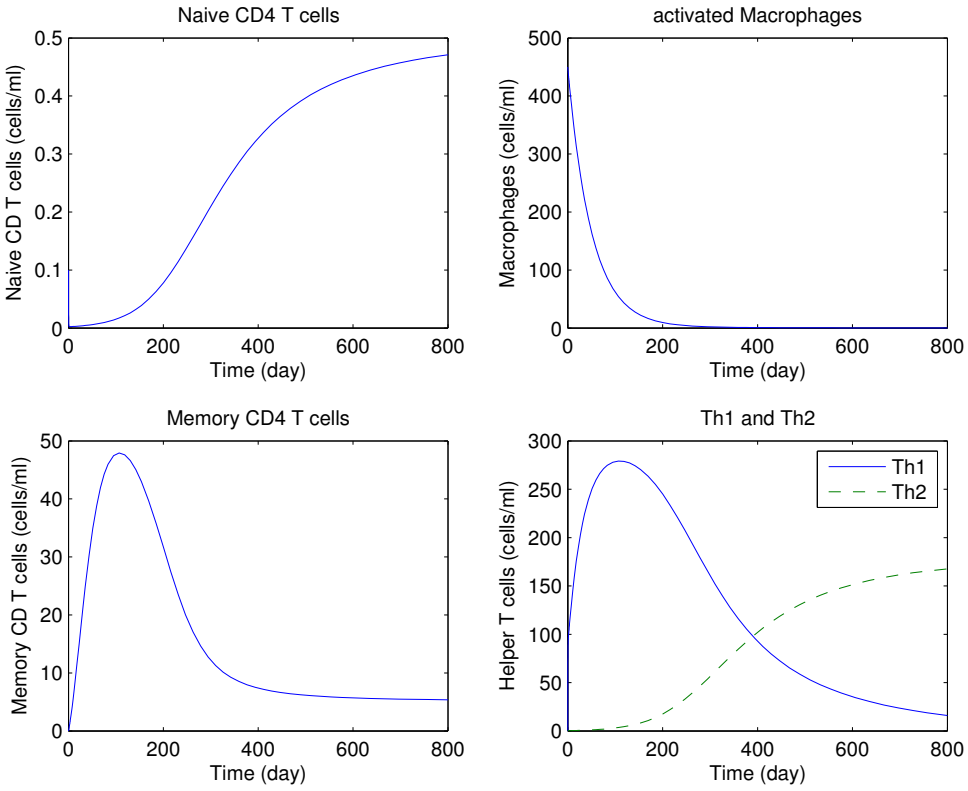

Figure 5.5: Systems dynamics for $\sigma_\Phi = 0.0001\text{day}^{-1}$. All other parameters as in Table 5.1.

Motivated by the differences of the system's dynamics in Figures 5.4 and 5.5 induced by changing parameter σ_Φ, we perform a bifurcation analysis by choosing σ_Φ as the bifurcation parameter. We are in particular interested to see how the value of σ_Φ influences the size of the memory CD4 T cell population.

Figure 5.6 shows the change in the memory CD4 T cell steady-state depending on the parameter σ_Φ. Below a certain threshold, $\sigma_{\Phi_c} \approx 1.333 \cdot 10^{-4}\text{day}^{-1}$, increasing the rate at which macrophages are recruited and activated by Th_1 cells does not impact the memory CD4 T cell steady-state. The rate at which macrophages are recruited and activated is not large enough to prevent the Th_1 cells and macrophages from going extinct over time. Therefore the memory cells at steady-state are just derived from the Th_2 cell population, whose size does not depend on the amount of macrophages available. Increasing the activation of macrophages further, thereby passing the threshold value, leads to a change in the dynamics of the system. There are enough macrophages to prevent Th_1 cells and macrophages from dying out and the memory cells now originate from both Th_1 and Th_2 cells. Since a higher activation rate of macrophages leads to more Th_1 cells being differentiated from naive CD4 T cells, the memory cell population increases as well as the activation rate of macrophages

increases.

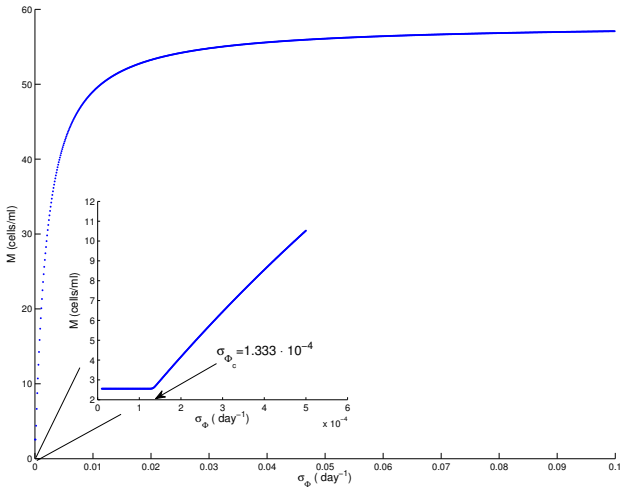

Figure 5.6: Bifurcation diagram showing the steady-state of memory CD4 T cells when σ_Φ is varied.

Next, we are interested in whether other parameters influence the amount of memory cells at steady-state. First, we look at the per capita rate δ_1 at which naive CD4 T cells differentiate into Th_1 cells. All other parameters are fixed at the values given in Table 5.1. The bifurcation diagram is given in Figure 5.7.

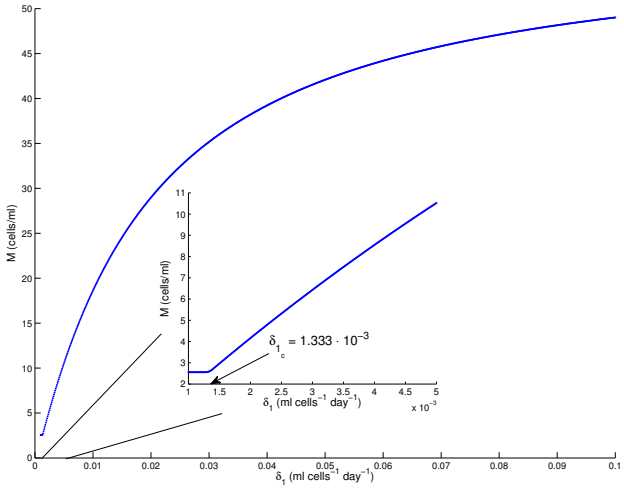

Figure 5.7: Bifurcation diagram showing the steady-state of memory CD4 T cells when δ_1 is varied.

Comparing Figures 5.6 and 5.7, we see that the bifurcation diagrams for σ_Φ and δ_1 have similar shapes, which is not astonishing considering that $\sigma_\Phi\delta_1$ appear together in the formulation of R_0 and $\overline{x}_3$.

Lastly, we consider d_1, the decay rate of Th_1 cells, as bifurcation parameter. We expect the bifurcation diagram to look different than the ones considered above, since R_0 is inversely proportional to d_1 but directly proportional to σ_Φ and δ_1. Therefore we expect the steady-state of coexistence of all cell populations, $\overline{x}_3$, in which the steady-state memory CD4 T cell population is dependent on d_1, to be stable for small parameter values d_1. Furthermore we expect steady-state $\overline{x}_1$, in which the populations of Th_1 cells and macrophages die out and the steady-state memory CD4 T cell population is independent of d_1, to be stable for large parameter values of d_1. The bifurcation diagram can be seen in Figure 5.8.

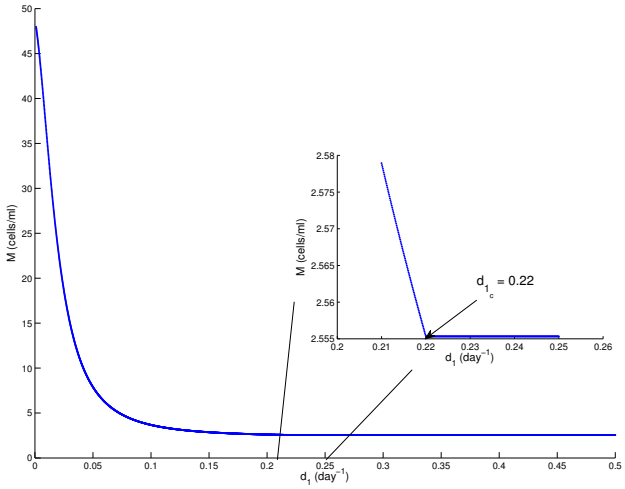

Figure 5.8: Bifurcation diagram showing the steady-state of memory CD4 T cells when d_1 is varied.

Indeed, comparing the bifurcation diagrams for parameters σ_Φ and δ_1 in Figures 5.6 and 5.7 with the bifurcation diagram for parameter d_1 in Figure 5.8, we can observe the predicted inverse behavior.

This tells us, that if the recruitment of macrophages or the differentiation rate of naive CD4 T cells into Th_1 cells are high, and if the decay rate of Th_1 cells is low, then the populations of Th_1 cells and macrophages survive, since their mutual promotion governs their decay. In this case the constant level of memory CD4 T reached over time is originating partly from Th_1 cells. Contrarily, for a large decay rate of Th_1 cells and either low differentiation rate of naive CD4 T cells into Th_1 cells or low activation rate of macrophages by Th_1 cells, the Th_1 cells decay faster than they can be reproduced. Hence they go extinct. In consequence, in this scenario, the memory cell population is not depending on characteristics of Th_1 or macrophage populations.

Next, we want to use our model to simulate the immune response following the boosting one year after the primary vaccination. The solid line in Figure 5.9 shows the simulation of the immune response following an initial vaccination with strain RB51 and boosting with strain RB51. To simulate the immune response in the first year following the primary vaccination, we choose $\sigma_\Phi = 0.0001$ and all other parameters and initial conditions as in Table 5.1. We then take the final state, in which the system is after 365 days, as the new initial conditions for the CD4 T cell subpopulations. Further, for the macrophages we choose the same initial condition as in the simulation of the primary vaccination to account for the application of the vaccine. The parameters chosen in the simulation of the immune response following boosting with RB51 are the same as the ones for the primary vaccination.

The dashed line in Figure 5.9 shows the simulation of the immune response following

the initial vaccination with strain 19 and boosting with strain RB51. Except for choosing $\sigma_\Phi = 0.001$ instead of 0.0001 in the simulation of the immune response following the primary vaccination, all parameters and initial conditions are chosen or determined as in the case, where for primary and booster vaccination strain RB51 is applied.

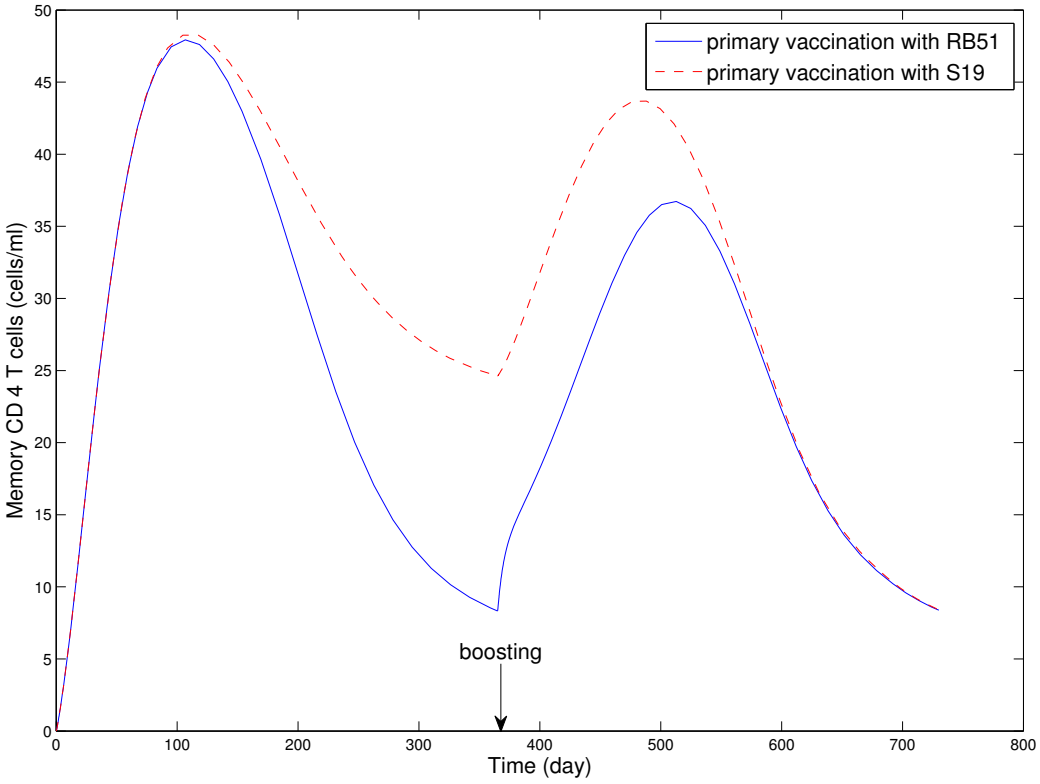

Figure 5.9: Simulation of vaccination with strain RB51 (solid line) or strain 19 (dashed line) and boosting with strain RB51

In both cases our model predicts that the memory cell population grows again after the application of the booster. This is followed by a contraction phase to a constant level. The differences between the two vaccination regimes consist of a higher memory CD4 T cell population persisting after the primary vaccination and a higher peak in memory CD4 T cells following the booster when strain 19 is applied as the primary vaccine compared to using strain RB51 in both vaccinations. Furthermore, the memory CD4 T cell population expands to approximately four times its size before the booster within the first months following the booster when the primary vaccine is strain RB51, compared to only approximately 1.7 times when first applying strain 19.

5.5 Discussion

We established a model that is able to reproduce two different patterns in the behavior of memory CD4 T cells seen in different vaccine trials. We derived an analytical value that defines the combination of parameters that account for low or high memory CD4 T cell levels in the long run following the vaccination. Interestingly, the behavior of memory CD4 T cells is correlated to different patterns for the temporal behavior of Th_1 and Th_2-type immune responses. For $R_0 > 1$ a predominant cellular, Th_1-type immune response in coexistence with a weaker anti-inflammatory, Th_2-type immune response can be observed together with a large steady-state memory CD4 T cell population. Conversely, for $R_0 < 1$ the Th_1 immune response is dominant shortly after vaccination but goes exist over time whereas the anti-inflammatory Th_2 immune response which is weak initially strengthens over time. In this case the steady-state memory CD4 T cell population is small as well.

We also used our model to simulate the memory CD4 T cell population after boosting. The model is able to reproduce the second peak in memory cells observed in the two vaccine trials.

We find that the rate σ_Φ at which Th_1 cells recruit and activate macrophages has, once above a certain threshold, a large impact on the size of the memory CD4 T cell population. It also influences the behavior of the cellular and anti-inflammatory immune responses. For values of σ_Φ below a certain threshold there is only a small population of memory cells developed. The size of this is independent of σ_Φ. Comparing that to our analytical results this corresponds to the steady-state in which the population of Th_1 effector cells and activated macrophages go extinct over time. Biologically that means, that there are not enough macrophages that can take up the bacteria and promote the differentiation of naive CD4 T cells into Th_1 effector cells, which in turn could again lead to more available macrophages. This leads to the extinction of both Th_1 cells and macrophages over time. To make up for the failure of the cellular immune response to clear the bacteria the body then starts to produce more and more Th_2 cells probably in an effort to fight the bacteria in an antibody-type response. If σ_Φ is increased above a certain threshold the mutual upregulation of macrophages and Th_1 cells allows for these cells to reach a positive equilibrium. As the parameter increases, the Th_2 response becomes small compared to the Th_1 response. This could indicate that phagocytosis of bacteria by macrophages during the cellular immune response leads to the clearance of most of the bacteria for which reason the anti-inflammatory immune response against free bacteria remains small. The amount of memory CD4 T cells developed depends on the number of Th_1 effector cells. Once above the threshold, a greater recruitment and activation rate of macrophages leads to an increase in Th_1 effector cells. Therefore the memory pool increases as well.

Similarly our model predicts, that once above a certain threshold, the amount of memory CD4 T cells at steady-state increases as the differentiation rate of naive CD4 T cells increases. In terms of biology that tells us, that when the differentiation rate of naive CD4 T cells into Th_1 cells is low, the mutual promotion of Th_1 cells and macrophages is not strong enough to prevent their dying off. But as more naive CD4 T cells differentiate into Th_1 cells, the Th_1

population becomes larger, thereby recruiting and activating more macrophages, that in turn lead to more Th_1 cells being produced. The strength of mutual promotion is large enough to prevent macrophages and Th_1 cells from extinction. Since in this case the memory CD4 T cell population depends on the amount of Th_1 cells, it increases as the Th_1 cell population increases.

The decay rate of Th_1 cells has an inverse influence on the amount of memory cells in the steady-state. If Th_1 cells decay fast, then this decay dominates the behavior of macrophages and Th_1 cells and they become extinct. Contrarily, if Th_1 cells decay slow, they persist in the system as well as macrophages.

Using the data from [13] we saw that after vaccination with strain 19 the level of memory CD4 T cells persisting long after vaccination is increased. Contrarily, after vaccination with strain RB51, the memory CD4 T cell population returns to its original size within a year after vaccination. Relating the immune response following strain 19 vaccination to the state in which our model predicts a high steady-state memory CD4 T cell population leads to the assumption that vaccination with strain 19, which is the more virulent of the two vaccines [4], triggers a strong pro-inflammatory, Th_1-type immune response. Moreover, it predicts a weak anti-inflammatory, Th_2-type immune response, which confirms that the anti-inflammatory cytokine IL-4 does not play a significant role in building up protection following S19 vaccination and RB51 boosting [14]. According to [14], the booster with strain RB51 after primary vaccination with strain 19 does not significantly enhance the immune response compared to just vaccinating with strain 19. This confirms our model's prediction that the memory CD4 T cell population persisting long time after the booster is not higher than before the booster. The behavior of memory CD4 T cells after primary vaccination with strain RB51 matches their behavior in the second possible pattern that our model predicts for the immune response. In this case after an initial peak of the pro-inflammatory immune response, the anti-inflammatory, Th_2-type immune response is dominant, whereas the inflammatory immune response goes extinct. This could implicate that a weaker trigger of the inflammatory immune response in vaccination with the less virulent strain RB51 [4] leads to the lower number of memory CD4 T cells persisting in the system. To validate these results further biological experiments need to be performed.

Chapter 6

Future work

Our model predicts a strong Th_1 response for values of σ_Φ, the rate at which macrophages are recruited and activated by Th_1 cells, large compared to the decay rate of Th_1 cells. A strong Th_1 response, and therefore a large value of σ_Φ, corresponds to a high memory CD4 T cell steady-state. Th_1 cells are commonly understood to be the main producers of IFN-γ. Looking at the two cohorts of cows, we see a high memory CD4 T cell steady-state in the cows first vaccinated with strain 19. So, for this cohort we expect a high IFN-γ production. Contrarily, for the cohort first vaccinated with strain RB51, which we relate to a low value of σ_Φ, we expect the Th_1 cells to peak in the beginning but to go extinct over time. So for times after the peak of Th_1 cells, the values of IFN-γ should be lower than for cows first vaccinated with vaccine strain RB51. We choose four cows, two good responding and two bad responding cows, of each cohort. In the left panel of Figure 6.1 we display the levels of IFN-γ for the good responding cows R6, R7 from the RB51 cohort and S13 and S15 from the S19 cohort. The right panel of Figure 6.1 shows the IFN-γ levels of bad responding cows R14, R17, S4 and S7. We can see, that before the booster, which is the time span we simulated, the levels of IFN-γ look as expected. After the initial peak, the IFN-γ level is greater in cows from the S19 vaccinated cohort than in cows from the RB51 vaccinated cohort.

Next, we take the same cows and compare the levels of Th_1 cells. The results are shown in Figure 6.2. Again we anticipate, that at least after some initial peak, the concentration of Th_1 cells in cows from the S19 vaccinated cohort is above the concentration in cows from the RB51 vaccinated cohort. When considering the data for the good responding cows, despite several missing measurements, it looks as if the cows from the cohort first vaccinated with strain 19 are expressing slightly more Th_1 cells than the ones from the other cohort. Contrarily the bad responding cows seem to show opposite behavior.

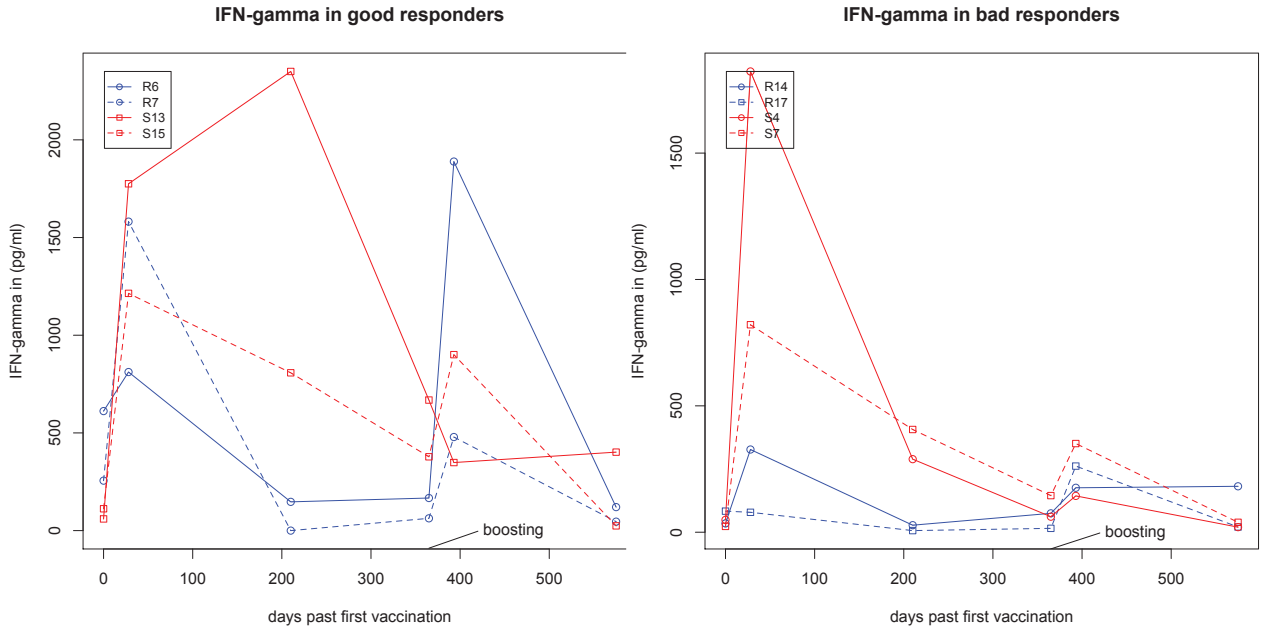

Figure 6.1: IFN-γ production of selected cows from both cohorts

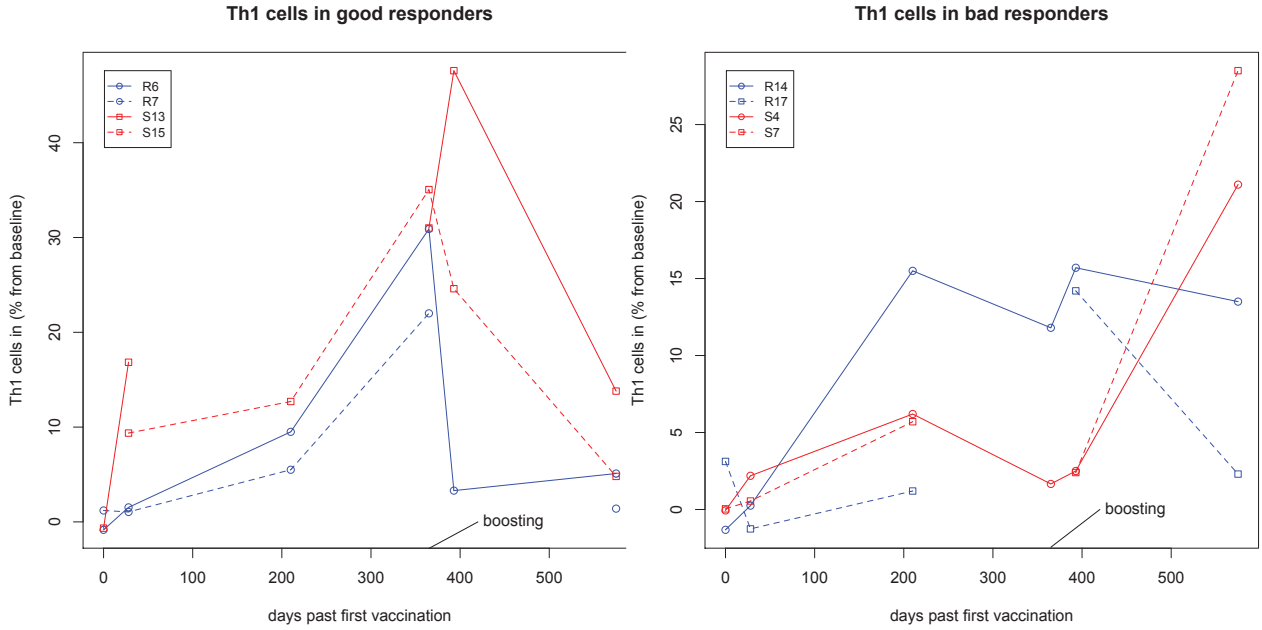

Figure 6.2: Th_1 cells in selected cows from both cohorts

Another cell that produces IFN-γ are CD8 T cells. The time evolution of this cell type for the same eight cows as in above investigations is displayed in Figure 6.3. The left panel shows the data for the good responders and the right panel the data for bad responding cows. The diagrams do not indicate a large population of IFN-γ producing CD8 T cells for either of the cows shortly after the vaccine is applied. We can therefore exclude them as the origin of the high IFN-gamma levels.

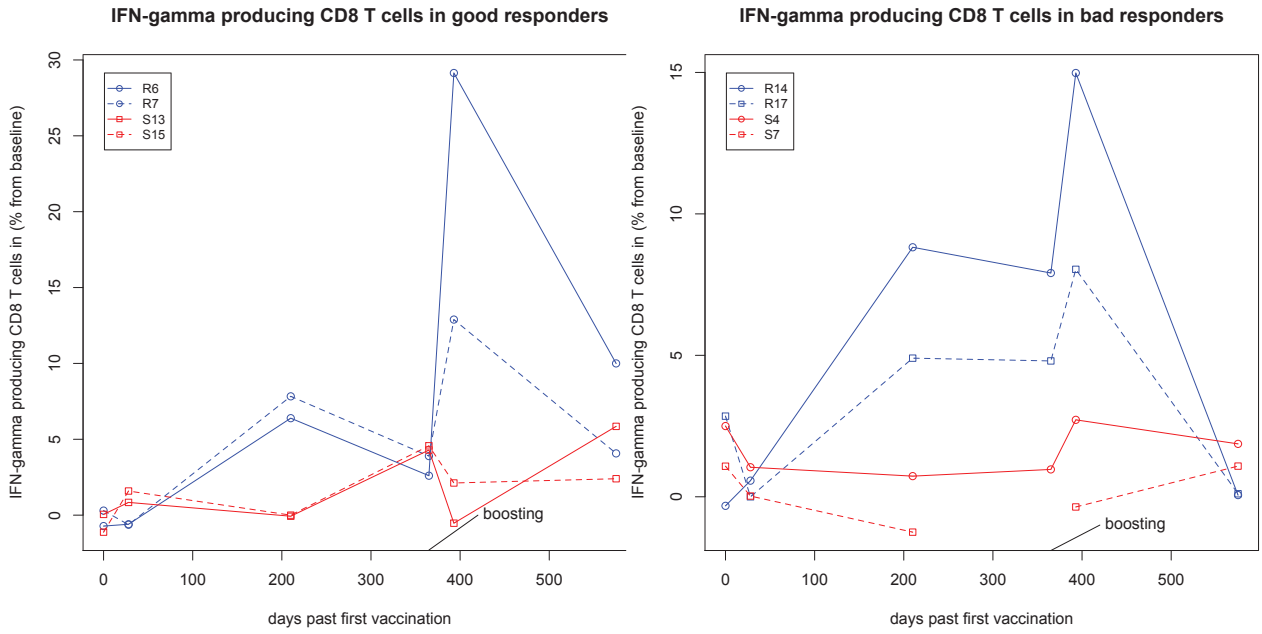

Figure 6.3: IFN-γ producing CD8 T cells in selected cows from both cohorts

Lastly, the data show that, for the good responding cows, the Th_1 cell populations increase significantly between 210 and 365 days after vaccination, whereas the IFN-γ levels decrease significantly in the same time frame, which is hard to explain biologically.

To address the puzzling dynamics of CD4, CD8 and IFN-γ populations, we aim to develop mathematical models that account for all known interactions.

Based on literature search we created diagrams for the different pathways of CD4, CD8 and B cells based on know cell-cell and cell-cytokine interactions. They are shown in Figures 6.4 to 6.6.

In these diagrams, red arrows indicate the differentiation of one cell type into another. Light blue arrows show that the differentiation, that the arrow is pointing at, depends on the availability of the resource at the origin of the arrow. Dark blue arrows signal the secretion of a cytokine by a cell population while yellow arrows indicate inhibition of either a production or a differentiation.

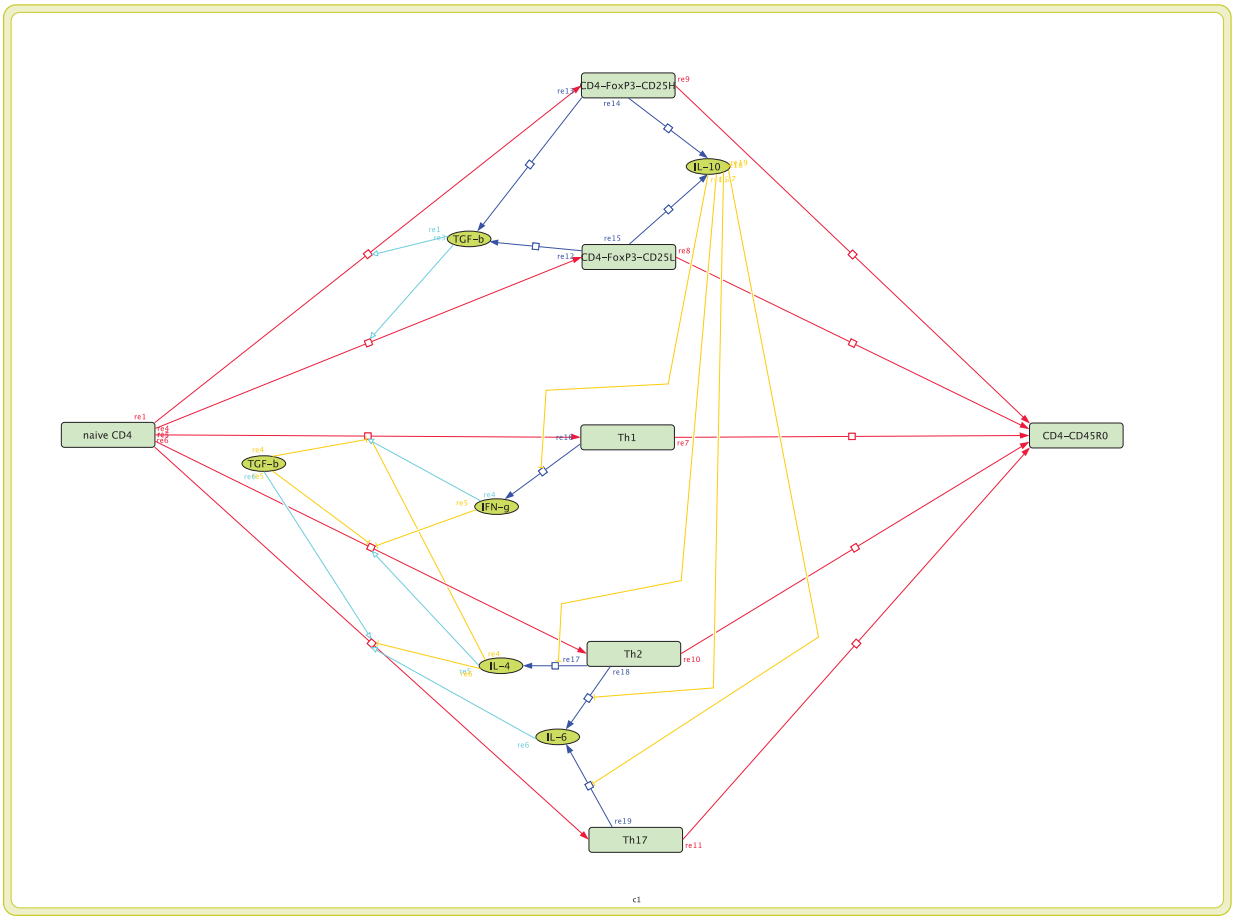

Figure 6.4: Interactions of CD4 T cell subpopulation and cytokines

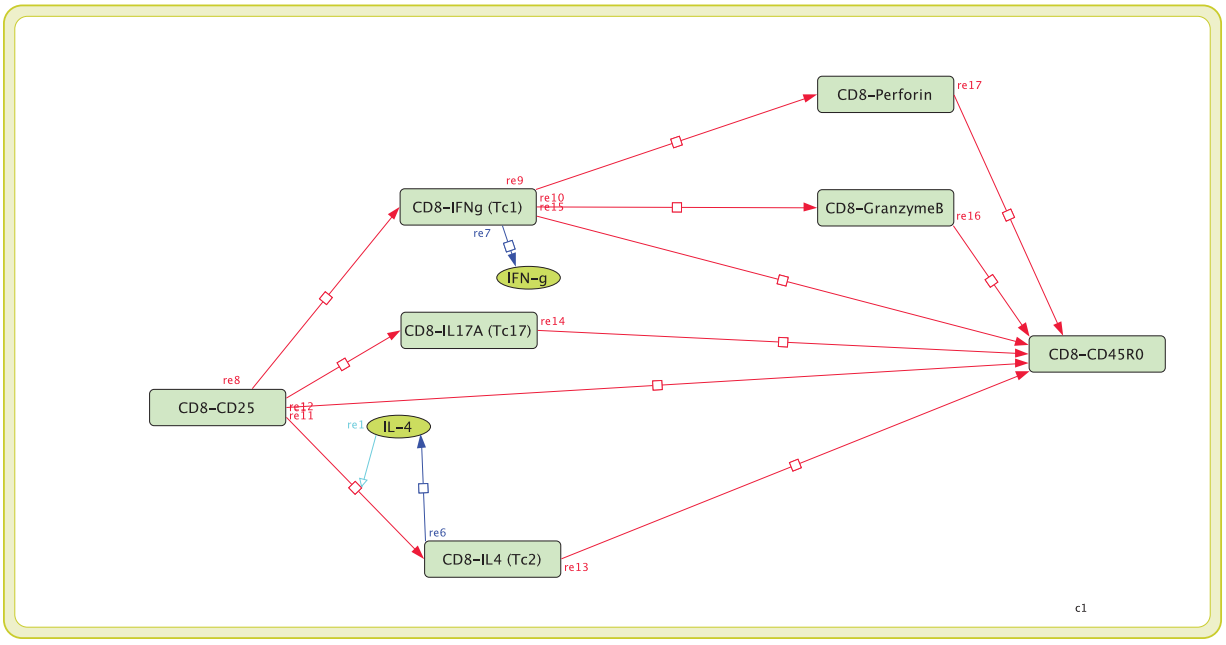

Figure 6.5: Interactions of CD8 T cell subpopulation and cytokines

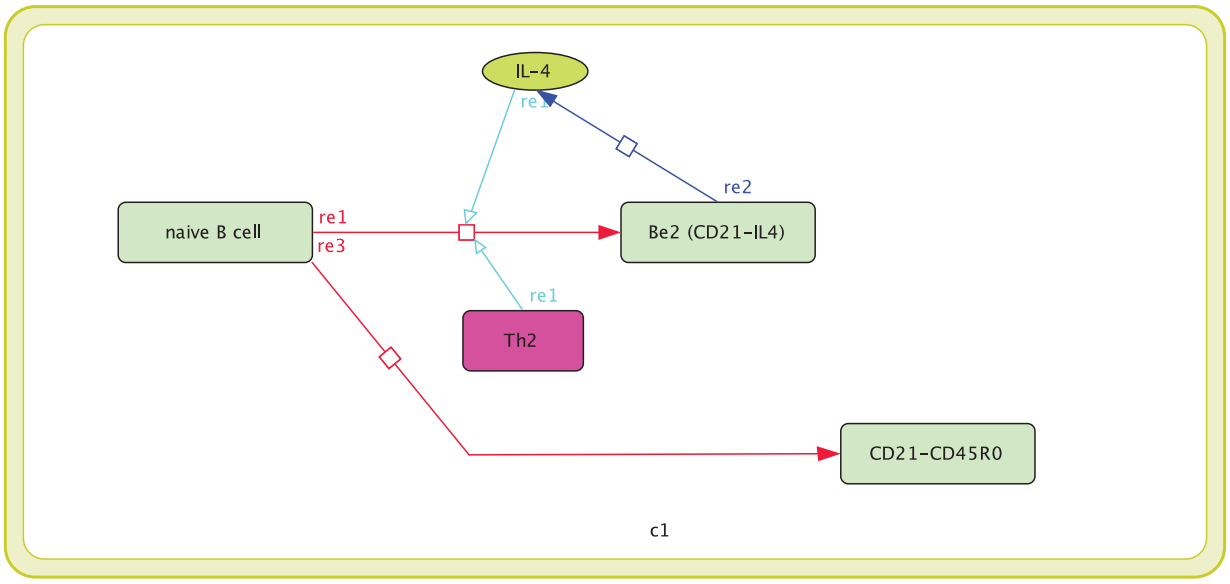

Figure 6.6: Interactions of B cell subpopulation and cytokines

We plan to develop models corresponding to these diagrams, and determine the effects

of cell interactions on IFN-γ production. The aim is to determine the parameter values that explain the IFN-γ evolution following vaccination and to predict whether additional variable nodes or arrow interactions are needed to explain the data in the two cow cohorts.

Chapter 7

Conclusion

In this thesis we investigated the differences between the immunological responses in cows following two vaccination regimes. In the first part of the thesis, we assessed what it means to have a positive response following vaccination by developing a distance measure for the goodness of response. We found that vaccination with strain 19 and boosting with strain RB51 gives better results than vaccination and boosting with strain RB51. However, the differences are not statistically significant. In the second part of the thesis, we developed a mathematical model of memory CD4 T cell development. We showed that the two different memory cell patterns observed in the two vaccines, expansion followed by positive equilibrium versus expansion followed by contraction, correlate with a Th_1 predominant, versus Th_2 predominant immune response, respectively. This prediction may be important when assessing the advantages and disadvantages of each vaccine usage.

Bibliography

[1] B. Alberts, A. Johnson, J. Lewis, and et al. *Biology of the Cell*. Garland Science, New York, 4 edition, 2002.

[2] L. Allen. *An Introduction to Mathematical Biology*. Pearson Education, Inc., Upper Saddle River, NJ, USA, 2007.

[3] E. Aparicio. Epidemiology of brucellosis in domestic animals caused by Brucella melitensis, Brucella suis and Brucella abortus. *Revue scientifique et technique (International Office of Epizootics)*, 32:53–60, 2013.

[4] E. Avila-Calderón, A. Lopez-Merino, N. Sriranganathan, S. Boyle, and A. Contreras-Rodríguez. A history of the development of Brucella vaccines. *BioMed Research International*, 2013, 2013.

[5] U. Behn, H. Dambeck, and G. Metzner. Modeling Th1-Th2 regulation, allergy and hyposensitization. In F. Bagnoli and S. Ruffo, editors, *Dynamical Modeling in Biotechnologies (Lectures presented at the EU Advanced Workshop, Torino, May27-June9,1996)*. World Scientific, Singapore, New Jersey, London, Hong Kong, 2001.

[6] U. Behn and R. Vogel. Th1-Th2 regulation and allergy: Bifurcation analysis of the non-autonomous system. In A. Deutsch, R. de la Parra, R. de Boer, O. Diekmann, P. Jagers, E. Kisdi, M. Kretschmar, P. Lansky, and H. Metz, editors, *Mathematical Modeling of Biological Systems, Volume II*. Birkhäuser, Boston, 2008.

[7] N. Bourbaki. *Elements of Mathematics Functions of a Real Variable*. Springer-Verlag Berlin Heidelberg, 2004.

[8] C. Cekic, D. Sag, Y. Day, and J. Linden. Extracellular adenosine regulates naive T cell development and peripheral maintenance. *JEM*, 210:2693–2706, 2013.

[9] V. Chellaboina, S. Bhat, W. Haddad, and D. Bernstein. Modeling and anlysis of mass-action kinetics. *IEEE Control Systems Magazine*, 2009.

[10] Y. Chien, C. Jan, H. Kuo, and C. Chen. Nationwide hepatitis B vaccination program in Taiwan: effectiveness in the 20 years after it was launched. *Epidemiological Reviews*, 28:126–135, 2006.

[11] L. Cosmi, L. Maggi, V. Santarlasci, and A. F. T helper cells pasticity in inflammation. *Cytometry Part A*, 85:36–42, 2014.

[12] N. Dalmia and A. Ramsay. Prime-boost apprroaches to tuberculosis vaccine development. *Expert review of vaccines*, 11:1221–1233, 2012.

[13] E. Dorneles. *Immune response of calves vaccinated with Brucella abortus S19 or RB51 and revaccinated with RB51.* PhD thesis, Universidade Federal de Minas Gerais, 2015.

[14] E. Dorneles, A. Teixeira-Carvalho, M. Araújo, G. Lima, O. Martins-Filho, N. Sriranganathan, and A. Lage. T lymphocytes subsets and cytokine pattern induced by vaccination against bovine brucellosis employing S19 calfhood vaccination and adult RB51 revaccination. *Vaccine*, pages 6034–6038, 2014.

[15] F. Gross, G. Metzner, and U. Behn. Mathematical modelling of allergy and specific immunotherapy: Th1-Th2-Treg interaction. *Journal of Theoretical Biology*, 269:70–78, 2010.

[16] Y. He, S. Reichow, S. Ramamoorthy, and et al. Brucella melitensis triggers time-dependent modulation of apoptosis and down-regulation of mitochondrion-associated gene expression in mouse macrophages. *Infection and Immunity*, 74:5035–5046, 2006.

[17] A. Hegazy, M. Peine, C. Helmstetter, I. Panse, A. Fröhlich, A. Bergthaler, L. Fatz, D. Pinschewer, A. Radbruch, and M. Löhning. Interferons direct Th2 cell reprogramming to generate a stable GATA-3^{+}T-bet^{+} cell subset with combined Th2 and Th1 cell functions. *Cell Press, Immunity*, pages 116–128, 2010.

[18] S. Jameson and D. Masopust. Diversity in T cell memory: An embarrassment of riches. *Immunity (Cell Press)*, 18:859–871, 2009.

[19] C. j. Janeway, P. Travers, M. Walport, and et al. *Immunobiology: The Immune System in Health and Disease.* Garland Science, New York, 5 edition, 2001.

[20] M. MacLeod, J. Kappler, and P. Marrack. Memory CD4 T cells: generation, reactivation and re-assignment. *Immunology*, 130:10–15, 2010.

[21] I. Magalhaes, D. Sizemore, R. Ahmed, S. Mueller, L. Wehlin, C. Scanga, F. Weichold, G. Schirru, P. MG, J. Goudsmit, S. Kühlmann-Berenzon, M. Spångberg, J. Andersson, H. Gaines, R. Thorstensson, Y. Skeiky, J. Sadoff, and M. Maeurer. rBCG induces strong antigen-specific T cell responses in rhesus macaques in a prime-boost setting with an adenovirus 35 tuberculosis vaccine vector. *PLoSone*, 3:e3790, 2008.

[22] G. Magombedze, S. Eda, and V. Ganusov. Competition for antigen between Th1 and Th2 responses determines the timing of the immune response switch during mycobacterium avium subspecies paratuberulosis infection in ruminants. *PLOS Computational Biology*, 10:e1003414, 2014.

[23] G. Magombedze, P. Reddy, S. Eda, and G. VV. Cellular and population plasticity of helper CD4+ cell responses. *Frontiers in Physiology*, 4:Article 206, 2013.

[24] J. Moran, R. Gonzlez-Polo, G. Soler, and J. Fuentes. Th1/Th2 cytokines: An easy model to study gene expression in immune cells. *CBE - Life Sciences Education*, 5:287–295, 2006.

[25] H. Peltola, O. Heinonen, M. Valle, M. Paunio, M. Virtanen, V. Karanko, and K. Canteli. The elimination of indigenous measels, mumps, and rubella from Finland by a 12-year, two-dose vaccination program. *The New England Journal of Medicine*, 331:1397–1402, 1994.

[26] S. Plotkin and S. Plotkin. A short history of vaccination. In S. Plotkin, W. Orenstein, and P. Offit, editors, *Vaccines*. Elsevier Inc., 4 edition, 2008.

[27] R Core Team. *R: A Language and Environment for Statistical Computing*. R Foundation for Statistical Computing, Vienna, Austria, 2014.

[28] R Core Team. *R: A Language and Environment for Statistical Computing*. R Foundation for Statistical Computing, Vienna, Austria, 2014.

[29] J. Richter, G. Metzner, and U. Behn. Mathematical modellinng in venom immunotherapy. *Journal of Theoretical Medicine*, 4:119–132, 2002.

[30] J. Sathiyaseelan, X. Jiang, and C. Baldwin. Growth of brucella abortus in macrophages from resistant and susceptible mouse strains. *Clinical and Experimental Immunology*, 121:289–294, 2000.

[31] C.-A. Siegrist. Vaccine immunology. In S. Plotkin, W. Orenstein, and P. Offit, editors, *Vaccines*. Elsevier Inc., 4 edition, 2008.

[32] H. Smits and M. Kadri. Brucellosis in India: a deceptive infectious disease. *Indian J Med Res*, 122:375–384, 2005.

[33] M. Stevens, S. Hennager, S. Olsen, and N. Cheville. Serological responses in diagnostic tests for brucellosis in cattler vaccinated with Brucella abortus 19 or RB51. *Journal of Clinical Microbiology*, 32, 1994.

[34] P. Waltman. *Competition Models in Population Biology*. Society for Industrial and Applied Mathematics, 1983.